

Zinc finger protein 180 induces an apoptotic phenotype by activating METTL14 transcriptional activity in colorectal cancer

LIANG XU^{1,2*}, XI-JIE CHEN^{2,3*}, QIAN YAN^{2,4*}, XIN-TAO LEI^{1*}, HAI-LING LIU¹,
JING-PING XU¹, WEI-TE SHANG¹, JING-LIN HUANG¹, ZHI-TING CHEN¹, XIAO-LI TAN¹,
HAN-JIE LIN¹, XIN-HUI FU¹, LI-SHENG ZHENG⁵, PING LAN^{2,4,6} and YAN HUANG^{1,7}

¹Department of Pathology, The Sixth Affiliated Hospital, Sun Yat-sen University, Guangzhou, Guangdong 510655, P.R. China;

²Guangdong Provincial Key Laboratory of Colorectal and Pelvic Floor Diseases, Guangdong Institute of Gastroenterology, The Sixth Affiliated Hospital, Sun Yat-sen University, Guangzhou, Guangdong 510655, P.R. China; ³Department of Gastrointestinal Surgery, The Sixth Affiliated Hospital, Sun Yat-sen University, Guangzhou, Guangdong 510655, P.R. China;

⁴Department of General Surgery (Colorectal Surgery), The Sixth Affiliated Hospital, Sun Yat-sen University, Guangzhou, Guangdong 510655, P.R. China; ⁵Department of Pathology, Guangdong Provincial People's Hospital (Guangdong Academy of Medical Sciences), Southern Medical University, Guangzhou, Guangdong 510080, P.R. China; ⁶State Key Laboratory of Oncology in South China, Guangzhou, Guangdong 510655, P.R. China; ⁷Biomedical Innovation Center, The Sixth Affiliated Hospital, Sun Yat-sen University, Guangzhou, Guangdong 510655, P.R. China

Received April 15, 2024; Accepted July 4, 2024

DOI: 10.3892/or.2024.8784

Abstract. Zinc finger protein 180 (ZNF180) is a multifunctional protein that interacts with nucleic acids and regulates various cellular processes; however, the function of ZNF180 in colorectal cancer (CRC) remains unclear. The present study investigated the role and function of ZNF180 in CRC, and aimed to reveal the underlying molecular mechanism. The results revealed that ZNF180 was downregulated in CRC tissues and was associated with a good prognosis in patients with CRC. Additionally, the expression of ZNF180 was downregulated by methylation in CRC. *In vivo* and *in vitro* experiments revealed that ZNF180 overexpression was functionally associated with the inhibition of cell proliferation and the induction of apoptosis. Mechanistically, chromatin immunoprecipitation-PCR and luciferase assays demonstrated that ZNF180 markedly regulated the transcriptional activity

of methyltransferase 14, N6-adenosine-methyltransferase non-catalytic subunit (METTL14) by directly binding to and activating its promoter region. Simultaneous overexpression of ZNF180 and knockdown of METTL14 indicated that the reduction of METTL14 could suppress the effects of ZNF180 on the induction of apoptosis. Clinically, the present study observed a significant positive correlation between ZNF180 and METTL14 expression levels, and low expression of ZNF180 and METTL14 predicted a poor prognosis in CRC. Overall, these findings revealed a novel mechanism by which the ZNF180/METTL14 axis may modulate apoptosis and cell proliferation in CRC. This evidence suggests that this axis may serve as a prognostic biomarker and therapeutic target in patients with CRC.

Introduction

Colorectal cancer (CRC) is one of the most common malignancies and ranks third among the leading causes of cancer-related death worldwide (1,2). Death due to CRC is mainly caused by disease recurrence and metastasis after surgery (3). Despite advances in treatment strategies, including improved surgical techniques and adjuvant therapy, the mortality rate among patients with CRC remains high due to high rates of metastasis and recurrence (4,5). Exploring the mechanisms that underlie the progression of CRC may accelerate the search for new diagnostic biomarkers and the development of effective therapeutic targets.

Zinc finger proteins (ZNFs) belong to a large group of proteins that bind to nucleic acids and perform various functions. The zinc finger domain is a common amino acid sequence motif that contains two cysteines and two histidines in specific positions that coordinate zinc. Okada *et al* (6) reported that the zinc finger transcription factor early growth

Correspondence to: Professor Yan Huang, Department of Pathology, The Sixth Affiliated Hospital, Sun Yat-sen University, 26 Yuancun Erheng Road, Guangzhou, Guangdong 510655, P.R. China
E-mail: huangy27@mail.sysu.edu.cn

Professor Ping Lan, Department of General Surgery (Colorectal Surgery), The Sixth Affiliated Hospital, Sun Yat-sen University, 26 Yuancun Erheng Road, Guangzhou, Guangdong 510655, P.R. China
E-mail: lanping@mail.sysu.edu.cn

*Contributed equally

Key words: colorectal cancer, prognostic model, zinc finger protein 180, methyltransferase 14, N6-adenosine-methyltransferase non-catalytic subunit, methylation, transcription factor

response gene-1 may be involved in inflammation caused by vascular injury and thrombosis. ZNF180 (also termed HHZ168) is a ZNF family member. It is a coded gene that regulates immune cell infiltration in melanoma cells and has an inverse relationship with plasminogen activator inhibitor-1 expression (7). Currently, research on ZNF180 is limited, particularly regarding its expression profile in CRC, and its association with tumor progression and prognosis remains unknown.

DNA methylation is a common epigenetic modification that regulates a variety of processes, such as differentiation, development, aging and tumorigenesis. Aberrant DNA methylation is one of the most common epigenetic aberrations in tumorigenesis (8). Aberrant DNA hypermethylation of CpG islands leads to silencing of genes involved in differentiation and the reactivation of stem cell-related genes (9). CpG methylation is primarily mediated by DNA methyltransferases (DNMTs), such as DNMT1, DNMT3a and DNMT3b (10). Hypermethylation of tumor suppressor genes is an early event in some solid tumors, and one of the earliest detectable features of neoplastic alterations associated with tumorigenesis (11,12). Several studies have identified specific DNA methylation sites for some genes, such as septin 9, as biomarkers for CRC (13-15). However, the association between ZNF180 and methylation, and its potential value in CRC screening and early detection remains to be further explored.

N6-methyladenosine (m^6A), one of the most common chemical modifications in eukaryotic mRNA, serves a crucial role in tumorigenesis and development. m^6A methylation is regulated by multiple genes and can be catalyzed by methyltransferases [e.g., methyltransferase 3/14/16, N6-adenosine-methyltransferase complex catalytic subunit (METTL3/14/16) 'writers'] or removed by demethylases (e.g., FTO and alkB homolog 5, RNA demethylase 'erasers'). In addition, it interacts with the m^6A binding proteins [e.g., YTH N6-methyladenosine RNA binding protein F1/2/3 (YTHDF1/2/3) and insulin-like growth factor 2 mRNA binding protein 1/2/3 'readers'] (16). METTL14 is a m^6A writing protein that is widely involved in the progression of major diseases (17). Studies have shown that METTL14 functions as a tumor suppressor in CRC (18), bladder cancer (19) and breast cancer (20); however, it has been reported to serve a role as a carcinogenic factor in thyroid cancer (21), pancreatic cancer (22) and leukemia (23).

The present study hypothesized that ZNF180 functions as a tumor suppressor gene, suppressing cell proliferation and inducing apoptosis in CRC cells. Therefore, the aim of this study was to investigate the molecular mechanisms underlying the function of ZNF180 in CRC.

Materials and methods

Cell lines and cell culture. The human cell lines 293T, HCT8, RKO, CACO2, SW480, SW620, LOVO, HCT116, HT29, DLD-1, HCT15, WIDR, SW48, COLO320 and LS174T, and the intestinal epithelial cell line HIEC-6 were cultured in Dulbecco's modified Eagle's medium (cat. no. C11995500BT; Gibco; Thermo Fisher Scientific, Inc.) supplemented with 10% FBS (cat. no. BS1614-105; BIOEXPLORER) at 37°C and 5% CO₂. The two cell lines with the highest efficiency of

overexpressing ZNF180 at the protein level (HCT116 and RKO) were selected for subsequent functional studies. All cell lines were purchased and certified from the American Type Culture Collection, with the exception of the HIEC-6 and CACO2 cell lines, which were obtained from the laboratory of Professor Ping Lan (The Sixth Affiliated Hospital, Sun Yat-sen University, Guangzhou, China).

Lentiviral production and cell transduction. Lentiviral-mediated cell transduction was performed as described previously (24). To prepare cells, several wells of target cells in the logarithmic growth phase and parallel control 293T cells were inoculated in a 24-well culture plate at a confluence of ~50%, 100 μ l medium was added to each well, and the cells were cultured until they became adherent. Notably, the optimal confluence of the cells for viral infection was ~70%. Lentiviruses were produced by mixing the ZNF180 overexpression plasmid (GV341) with 3x Flag-tagged ZNF180 (Shanghai GeneChem Co., Ltd.) and psPAX1 and pMD2.G packaging plasmids (3rd generation system) (ratio, 20 μ g:15 μ g:10 μ g; total, 45 μ g plasmid/10-cm dish) with Lipofectamine® 3000 (cat. no. L3000015; Invitrogen; Thermo Fisher Scientific, Inc.) at room temperature for 15 min. Subsequently, this mixture was used to transfect 293T cells at 37°C for 12 h and the medium was then changed. Lentiviruses were harvested 48 h after transfection, and filtered through a 0.22- μ m filter (MilliporeSigma). Subsequently, the target cells were transduced with lentiviruses (MOI=10) at 37°C for 12 h and were then cultured in medium. After 3 days, the medium was replaced with medium containing 2 mg/ml puromycin (cat. no. T19978; TargetMol Chemicals, Inc.) for 7 days. After 11 days, the subsequent experiments were carried out.

Small interfering (si)RNA transfection. The negative control siRNA (NC), METTL14 si#1 and si#2 were purchased from Guangzhou IGE Biotechnology Co., Ltd. The sequences were as follows: NC, sense 5'-UUCUCCGAACGUGUC ACGUTT-3', antisense 5'-ACGUGACACGUUCGGAGA ATT-3'; METTL14 si#1, sense 5'-GAACCUGAAAUUGGC AAUAUATT-3', antisense 5'-UAUAUUGCCAAUUCAGG UUCTT-3'; METTL14 si#2, sense 5'-GCUUACAAAUAG CAACUACAATT-3', antisense 5'-UUGUAGUUGCUAUUU GUAAGCTT-3'. Transient transfections of CRC cells were performed as described previously (25). Briefly, 60 pmol siRNA in Opti-MEM (cat. no. 31985070; Gibco; Thermo Fisher Scientific, Inc.) was mixed with Lipofectamine RNAiMAX Reagent (cat. no. 13778150; Invitrogen; Thermo Fisher Scientific, Inc.) and incubated at room temperature for 5 min. Subsequently, the mixture was added to the cells and incubated at 37°C for 12 h. A total of 4 days post-transfection, the subsequent experiments were performed.

Western blotting. Pre-chilled RIPA lysis buffer (cat. no. P0039; Beyotime Institute of Biotechnology) supplemented with phosphatase inhibitors (cat. no. P1009; Beyotime Institute of Biotechnology) was used for protein extraction. The BCA protein assay kit (cat. no. P10012S; Beyotime Institute of Biotechnology) was used for protein determination. Subsequently, 20 μ g proteins were loaded per lane, separated by SDS-PAGE on 10% gels and were transferred to 0.45- μ m

PVDF membranes (cat. no. FFP39; Beyotime Institute of Biotechnology). The membranes were blocked using 5% non-fat milk (cat. no. P0216; Beyotime Institute of Biotechnology) diluted in TBS-1% Tween 20 (TBST) at room temperature for 1 h, and were then incubated with primary antibodies (1:1,000) at 4°C overnight, followed by incubation with secondary antibodies (1:5,000) at room temperature for 1 h. A chemiluminescence reagent (cat. no. MA0186; Dalian Meilun Biology Technology Co., Ltd.) was used to visualize the proteins. Standard western blotting procedures were performed as described previously (26). The following antibodies were used in the present study: Anti-ZNF180 (cat. no. bs-8485R; BIOSS), anti-GAPDH (cat. no. 6004-1-Ig; Proteintech Group, Inc.), anti- β -actin (cat. no. 66009-1-Ig; Proteintech Group, Inc.), anti-METTL14 (cat. no. 26158-1-AP; Proteintech Group, Inc.), anti-PARP (cat. no. 9542S; Cell Signaling Technology, Inc.), anti-cleaved-PARP (cat. no. 5625S; Cell Signaling Technology, Inc.), and anti-mouse (cat. no. 7076; Cell Signaling Technology, Inc.) and anti-rabbit (cat. no. 7074; Cell Signaling Technology, Inc.) peroxidase-conjugated secondary antibodies.

RNA isolation and reverse transcription-quantitative PCR (RT-qPCR). Total RNA was isolated from cultured cell lines and tissues using TRIzol® reagent (Invitrogen; Thermo Fisher Scientific, Inc.), and was reverse transcribed using a cDNA Synthesis Kit (cat. no. R223-01; Vazyme Biotech Co., Ltd.), performed according to the manufacturer's protocol. qPCR was performed using a ChamQ Universal SYBR qPCR MasterMix (cat. no. Q711-02; Vazyme Biotech Co., Ltd.) according to manufacturer's protocol: 95°C for 30 sec; followed by 40 cycles at 95°C for 3 sec and 60°C for 10 sec; and a final melt curve stage. The relative expression levels of the target genes were calculated as $2^{-\Delta\Delta C_q}$ (27) (C_q of β -actin or GAPDH minus the C_q of the target gene). The sequences of the qPCR primers used for amplification were as follows: β -actin, forward 5'-CACCATTGGCAATGAGCGGTTC-3', reverse 5'-AGG TCTTTGCGGATGTCCACGT-3'; GAPDH, forward 5'-GTC TCCTCTGACTTCAACAGCG-3', reverse, 5'-ACCACCCTG TTGCTGTAGCCAA-3'; ZNF180, forward 5'-TGGAAGAGC AGGATGAGAAGCC-3', reverse, 5'-GATGGTCAGAGACCC AGTGTCT-3'; METTL14, forward 5'-CTGAAAGTGCCG ACAGCATTGG-3', reverse 5'-CTCTCCTTCATCCAGATA CTTACG-3'.

Immunofluorescence (IF). A total of 2×10^5 cells were cultured in a cell culture dish for 24 h, after which they were fixed onto slides with 4% paraformaldehyde for 15 min at room temperature, and then washed in PBS three times (3 min/wash). Subsequently, the cells were permeabilized with 1% Triton X-100 for 20 min at room temperature, followed by blocking with 10% goat serum (cat. no. I5256, Sigma-Aldrich; Merck KGaA; diluted in TBST) for 1 h at room temperature. The cells were then incubated with the following primary antibodies [1:200; diluted in QuickBlock buffer (cat. no. P0256; Beyotime Institute of Biotechnology)]: ZNF180 (cat. no. NBP1-92613; Novus Biologicals, Inc.) METTL14 (cat. no. 26158-1-AP; Proteintech Group, Inc.) and Ki67 (cat. no. CL594-27309; Proteintech Group, Inc.) at 4°C overnight, and with fluorescent secondary antibodies [(1:1,000; diluted in dilution buffer (cat. no. I917953, Macklin, Inc.)] at room temperature for

1 h. The following secondary antibodies were used: Goat anti-Rabbit IgG (H+L) cross-adsorbed secondary antibody with Alexa Fluor™ 594 (cat. no. A-11012; Thermo Fisher Scientific, Inc.) and Alexa Fluor™ 488 (cat. no. A-11008; Thermo Fisher Scientific, Inc.). The nuclei of the cells were stained with DAPI and a fluorescence microscope (IX73; Olympus Corporation) was used to visualize the cells.

Cell cycle analysis. After centrifugation at 1,000 x g for 5 min at room temperature, the supernatant removed and 1 ml PBS was added to the cells in an ice bath for resuspension. The cells were then transferred to a 1.5-ml microcentrifuge tube, centrifuged at 1,000 x g for 5 min at 4°C, the supernatant was removed and the cells (in 50 μ l) were washed twice with PBS, and resuspended in PBS containing 50 μ g/ml PI and 0.1 mg/ml RNase A (cat. no. C1052; Beyotime Institute of Biotechnology). After 30 min of incubation at 37°C in the dark, the cells were measured by flow cytometry (CytoFLEX S; Beckman Coulter, Inc.) and analyzed by software (CytExpert 2.4; Beckman Coulter, Inc.).

Human tissue samples. The present study included patients diagnosed with CRC between 2013 and 2020 at The Sixth Affiliated Hospital, Sun Yat-sen University (SYSU6; Guangzhou, China); also known as the SYSU6 cohort (n=244). Patient data were extracted from pathology report records. Only those patients with CRC who had complete clinical information and underwent surgery were selected. The average age of the patients recruited was ~56.7 years (range, 20-90 years), 41% of patients were women and 59% were men. To compare the ZNF180 and METTL14 levels among normal and tumor tissues, 24 CRC patient tissue samples and 24 matched normal tissues were obtained from the SYSU6 cohort (among them, 12 paired tissues were used for qPCR, and 24 paired tissues were used for western blot). In addition, ZNF180 levels were measured in the remaining formalin-fixed paraffin-embedded 220 CRC tissue sections from the SYSU6 cohort by immunohistochemistry (IHC). A total of 40 CRC tissues (from these 220 formalin-fixed paraffin-embedded tissues) that had both tumor cells and normal cells were used to detect the expression levels of ZNF180 and METTL14 by IHC.

IHC. Sections were fixed with 10% neutral buffered formalin at room temperature for 20 h and hydrated in a descending series of ethanol. All tissues were embedded in paraffin and cut into 3- μ m sections. Antigen retrieval was performed in 500 ml 0.01 M citrate buffer (pH=6.0; cat. no. 420901; Biolegend, Inc.) in a microwave for 10 min. After rinsing under cold tap water for 10 min, the sections were incubated for 10 min at room temperature with 10% serum blocking solution (cat. no. ZLI-9056; OriGene Technologies, Inc.). Subsequently, the sections were incubated with the following primary antibodies: ZNF180 (cat. no. NBP1-92613; Novus Biologicals, Inc.) and METTL14 (cat. no. 26158-1-AP; Proteintech Group, Inc.) in a 1:400 dilution in dilution buffer (cat. no. ZLI-9030; OriGene Technologies, Inc.) at 4°C for 12 h. The sections were then incubated for 10 min at room temperature with a biotinylated secondary antibody (cat. no. PV-9000-1; OriGene Technologies, Inc.) and for 10 min at room temperature with a streptavidin-enzyme conjugate (cat. no. PV-9000-2; OriGene

Technologies, Inc.), and for 2 min at room temperature with a substrate-chromogen mixture (cat. no. PV-9000-3; OriGene Technologies, Inc.). A light microscope (BX53; Olympus Corporation) was used to visualize the cells. For each tissue, a proportional score and an intensity score were determined. The proportional score was classified as: 0, no staining; 1, 1-10% stained cells; 2, 11-50% stained cells; 3, 51-80% stained cells; 4, 81-100% stained cells. The intensity score represents the intensity of cytoplasmic and membranous staining of positive cells, as follows: 0, no staining; 1, weak staining; 2, moderate staining; 3, strong staining.

Hematoxylin and eosin staining. Sections were fixed with 10% neutral buffered formalin at room temperature for 20 h and hydrated in a descending series of ethanol. All tissues were embedded in paraffin and cut into 3- μ m sections. Sections were deparaffinized and rehydrated in xylene and a descending series of ethanol. Subsequently, the sections were incubated with hematoxylin stain (cat. no. C0105S-1; Beyotime Institute of Biotechnology) for 3 min and 0.5% eosin (cat. no. C0105S-2; Beyotime Institute of Biotechnology) for 30 sec. The cells were mounted using Permount mounting medium (cat. no. ZLI-9516; OriGene Technologies, Inc.) after staining. A light microscope (BX53; Olympus Corporation) was used to visualize the cells.

Ethical statement. The present study involving human samples was approved by the Institutional Review Board of SYSU6 (approval no. 2021ZSLYEC-228), and complied with The Declaration of Helsinki (World Medical Association Declaration of Helsinki 2013). All patients provided written informed consent to allow their electronic medical records to be used for cancer research voluntarily during their first visit to the hospital, and data were anonymized at the beginning of statistical analyses to protect patients' privacy. All patients provided consent for their tissues to be used in medical research

DNA methylation. HCT116 and RKO cells were treated with 10 and 20 μ M 5-azacytidine (5-AzaC) (cat. no. S1782; Selleck Chemicals) for ~48 h. 5-AzaC is a DNA methyltransferase, which is commonly used for DNA methylation research. Cells were harvested within 3 days of treatment with 5-AzaC, total RNA was isolated for RT-qPCR and proteins were extracted for western blotting.

5-Ethynyl-20-deoxyuridine (EdU) staining. The EdU solution (cat. no. C0071S; Beyotime Institute of Biotechnology) was proportionally diluted with complete cell medium to prepare an appropriate amount of 2X EdU working solution with a final concentration of 50 μ M; briefly, 500 μ l dilution buffer and 500 μ l EdU working solution (1:1) were added to a 6-well plate, mixed evenly and incubated at 37°C for 6-7 h to achieve a final concentration of 50 μ M. For EdU staining, the medium was removed from cells and they were washed in PBS three times (5 min/wash), before being washed with PBS containing 3% BSA (cat. no. ST023; Beyotime Institute of Biotechnology) at room temperature. The cells were then permeabilized in PBS containing 0.5% Triton X-100 for 20 min at room temperature, and, after washing them with 3% BSA solution, the Click-iT EdU solution was added to the cells for 30 min at

room temperature; the nuclei were stained with Hoechst 33342 (cat. no. C0071S-6; Beyotime Institute of Biotechnology). Subsequently, DNA synthesis was observed under a confocal microscope.

Cell apoptosis detection. Apoptosis was assessed by Annexin V and PI staining using the Annexin V apoptosis detection kit (cat. no. C1062; Beyotime Institute of Biotechnology). Briefly, HCT116 and RKO vector and ZNF180-overexpression groups were treated with 5-fluorouracil (5-FU; 0, 10 or 20 μ M; cat. no. F6627; Sigma-Aldrich; Merck KGaA) diluted in DMSO. All cells were collected after treatment with 5-FU at 37°C for 2 days. Cells were washed twice with PBS and resuspended in binding buffer (500 μ l, 5×10^5 cells). Annexin V (5 μ l) and PI (5 μ l) were then added to the cells and incubated for 15 min at room temperature in the dark. The cells were measured by flow cytometry (CytoFLEX S; Beckman Coulter, Inc.) and analyzed using CytExpert 2.4 software (Beckman Coulter, Inc.).

Chromatin immunoprecipitation (ChIP) assay. ChIP was performed using the SimpleChIP® Enzymatic Chromatin IP Kit (cat. no. 9003S; Cell Signal Technology, Inc.), according to the manufacturer's protocol. First, DNA extracted from lysed cells was digested into 10-1,000 bp fragments using a micrococcal nuclease. For ZNF180-overexpressing HCT116 cells, a Flag antibody (cat. no. F1804; Sigma-Aldrich; Merck KGaA) was used to pull down ZNF180 protein (overexpression plasmid with 3x Flag-tagged ZNF180); normal rabbit IgG antibody (cat. no. 2729; Cell Signaling Technology, Inc.) was used as a negative control and Histone H3 rabbit monoclonal antibody was used as a positive control (cat. no. 4620; Cell Signaling Technology, Inc.). An anti-Flag antibody, and protein A and G magnetic beads were then added to the lysate and immunoprecipitated over 12 h. The enriched chromatin was then eluted for standard PCR followed by agarose gel electrophoresis (cat. no. DYCP-31CN; Beijing Liuyi Biotechnology Co., Ltd.) on a 1% agarose gel (cat. no. BS081; Biosharp Life Sciences), which was visualized using Gel-green (cat. no. D0143; Beyotime Institute of Biotechnology). The specific primers of METTL14 used for ChIP-PCR were: sense: 5'-GGCGCAACAGATCCCTTACT-3', antisense: 5'-CTCAGTAGAGAC TTCCGGCG-3'. The standard PCR reaction program was as follows: Initial denaturation at 95°C for 5 min; followed by 34 cycles of denaturation at 95°C for 30 sec, annealing at 62°C for 30 sec and extension at 72°C for 30 sec; and a final extension step at 72°C for 5 min. In addition, RT-qPCR was performed as aforementioned.

Cell proliferation assay. The colorimetric MTS assay (cat. no. G3580; Promega Corporation) was performed to determine cancer cell proliferation. Briefly, cells were seeded into 96-well plates (1,000 cells/well) and were incubated at 37°C for 6 days. Subsequently, a mixed solution of MTS and phenazine ethosulfate (20:1 ratio) was added to each well and incubated for a further 4 h. A microplate reader was then used to determine the absorbance value at 490.

Animal experiments. To generate ZNF180-overexpressing tumor xenografts, male BALB/c athymic nude mice

(GemPharmatech Co., Ltd.) (age, 4 weeks; weight, 12–14 g) were randomly divided into the vector and ZNF180-overexpression groups (n=12 mice each). The mice were housed under the following conditions: Temperature, 25°C; humidity, 60%; 12-h light/dark cycle; *ad libitum* access to food and water that was changed three times every week). HCT116 cells (2x10⁶ cells/tumor in 100 μ l DMEM) were injected subcutaneously into the right flanks of the nude mice. For inoculation, the needle was inserted under the skin (~1 cm deep) and was slid left and right several times, so that the cells were seeded into clumps and to reduce an overflow of cell suspension from the injection site. The tumor diameter was measured every 2–4 days after tumor establishment. The humane endpoint was that the tumor diameter of the mice should not exceed 1.5 cm. A total of 11 days after the injection of tumor cells, the mice were euthanized using CO₂ followed by cervical dislocation; initially, CO₂ was released at 30% chamber volume/min, but was increased to 50% chamber volume/min once the mice lost consciousness. CO₂ flow was maintained for >60 sec following respiratory arrest, followed by cervical dislocation to confirm the mice were euthanized. All animal experiments were approved by the Institutional Animal Care and Use Committee of SYSU6 (approval no. IACUC-2023101301).

Wound healing assay. HCT116 cells were seeded into 6-well plate and cultured to 90% confluence. Subsequently, serum was removed from the medium and the cells were cultured for 24 h before wound generation, after which, a sterile 200- μ l pipette tip was used to create an artificial wound in each 6-well plate and the floating cells were removed by washing with PBS. The corresponding images were captured at 0 and 24 h using an inverted light microscope (IX73; Olympus Corporation).

Transwell assay. For the Transwell migration assay, 5x10⁴ cells in 200 μ l serum-free DMEM were added to uncoated cell culture inserts (pore size 8 μ m; cat. no. 3428; Corning, Inc.) in a 24-well plate. In addition, 800 μ l complete medium containing 10% FBS was added to the lower chamber of the 24-well plate. The cells were incubated at 37°C (5% CO₂ and 90% humidity) for 22 h, and then stained with 1% crystal violet (cat. no. T1343L; TargetMol Chemicals, Inc.) at room temperature for 4 h and examined under an inverted light microscope (IX73; Olympus Corporation).

Luciferase assay. Briefly, 293T cells were seeded into 96-well plates at a density of 5,000 cells/well. The cells were then co-transfected with a *Renilla* luciferase plasmid (GemPharmatech Co., Ltd.), a firefly luciferase plasmid containing METTL14 promoter (GemPharmatech Co., Ltd.), and the aforementioned ZNF180 overexpression plasmid using the Roche X-tremeGENE™ HP DNA (cat. no. 6366546001; MilliporeSigma), according to the manufacturer's protocols, with three replicates for each test. Plasmid luciferase activities were normalized against the *Renilla* luciferase activity of the co-transfected internal control plasmid. Cells were harvested 48 h post-transfection, and luciferase activities were measured using the Dual-Luciferase Reporter Assay System (cat. no. E1910; Promega Corporation). The METTL14 promoter sequence is listed in Table SI.

Data source. The Cancer Genome Atlas (TCGA) RNA-seq transcriptome data and clinical information were obtained from TCGA database (<https://portal.gdc.cancer.gov>). The GSE39582 (28) and GSE87211 datasets (29) were retrieved from the Gene Expression Omnibus database (<http://www.ncbi.nlm.nih.gov/geo/>). The raw data were processed using the R packages GEOquery (<https://bioconductor.org/packages/release/bioc/html/GEOquery.html>) and Stringr (<https://cran.r-project.org/web/packages/stringr/index.html>). The mRNA expression levels of ZNF180 and METTL14 data in numerous CRC cell lines were obtained the DepMap portal (<https://depmap.org/portal/>). The CpG islands of the ZNF180 promoter were searched for using the UCSC Genome Browser (<http://www.genome.ucsc.edu>).

Risk signature construction and validation. Univariate Cox regression and Kaplan-Meier (KM) analysis using the survival R package (<https://cran.r-project.org/web/packages/survival/index.html>) were performed to identify genes associated with patient overall survival (OS) time from TCGA and GSE39582 datasets. Only when the P-values of both analysis methods were ≤ 0.05 were the genes included in the next step. The intersecting genes, identified by univariate Cox regression and KM analysis from TCGA and GSE39582 datasets were then analyzed by least absolute shrinkage and selection operator (LASSO) regression analysis using the glmnet R package (<https://cran.r-project.org/web/packages/glmnet/index.html>) in TCGA database to narrow the range of prognosis-related genes. Subsequently, the Akaike information criterion (AIC) method of multivariate Cox regression analysis was performed using the survival package to establish an optimal risk signature based on linear integration of the regression coefficient obtained from the multivariate Cox regression analysis and the expression level of the selected genes. The risk score was computed as follows:

$$\text{Risk score} = \sum_{i=1}^N (\text{Coef}_i * \text{Expi})$$

where Expi is the expression value of the genes and Coef_i is the corresponding regression coefficient calculated by multivariate Cox regression analysis. TCGA data were used as the training cohort and GSE39582 data were used as the validation cohort.

Statistical analysis. All *in vitro* experiments were repeated three times. Statistical analysis was performed using SPSS version 26 (IBM Corporation). Continuous variables are presented as the mean and standard deviation (SD), whereas categorical variables are presented as frequencies. The significance between two different groups of continuous variables was assessed using unpaired Student's t-test or paired Student's t-test, whereas the significance between the proportions of different groups was assessed using χ^2 test. The significance among multiple groups was assessed using one-way ANOVA for parametric data and the Scheffe post hoc test. KM analysis with log-rank test was used to compare the survival rates of each group. Multivariate analysis was conducted for the variables that were significantly associated with disease-free survival (DFS) in the

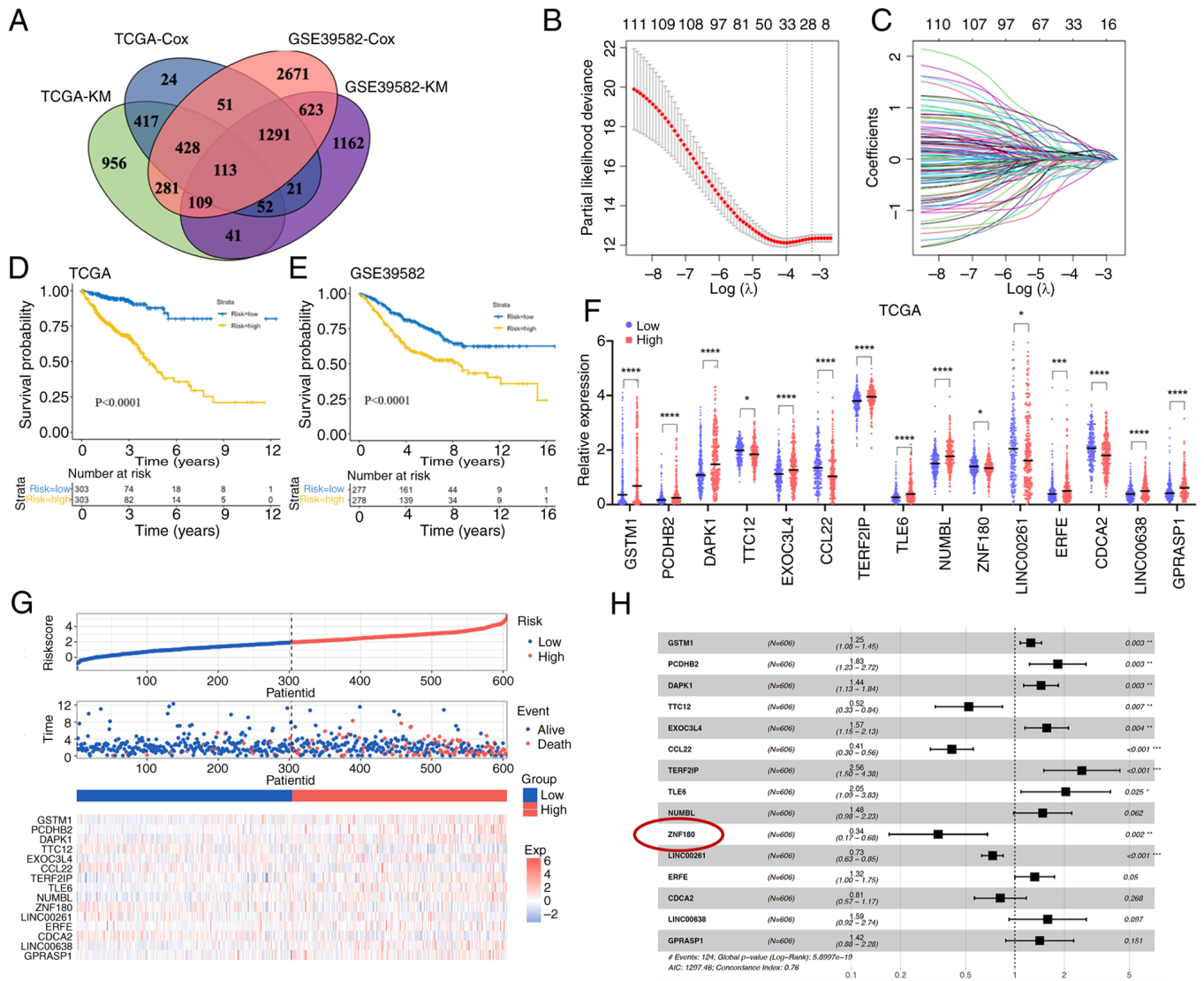


Figure 1. Identifying prognostic genes for developing a risk model. (A) Intersecting genes associated with colorectal cancer prognosis in TCGA and GSE39582 databases. (B) LASSO coefficient profiles of the 113 genes in TCGA data set. (C) Selection of the optimal parameter (λ) in the LASSO model. KM curves of the prognostic signature in (D) TCGA and (E) GSE39582 cohorts (analyzed using log-rank test). (F) Differential expression of the 15 genes in TCGA between different groups. *P<0.05, ***P<0.001, ****P<0.0001. (G) Distribution of risk score, survival duration and status of patients, and a heatmap of the 15 genes in the classifier. (H) A total of 15 genes were chosen for establishing a prognosis signature. The red circle indicates the target gene ZNF180. *P<0.05, **P<0.01, ***P<0.001. TCGA, The Cancer Genome Atlas; LASSO, least absolute shrinkage and selection operator; KM, Kaplan-Meier.

univariate Cox regression model, using the Cox proportional hazards regression model. Hazard ratios (HRs) and 95% confidence intervals were provided for the multivariate analysis. The correlation between two groups was evaluated using Pearson's correlation analysis (two-tailed). Unless specifically stated, all statistical tests were two-sided, and P<0.05 was considered to indicate a statistically significant difference.

Results

A total of 15 prognosis-related genes were identified to develop a risk model. To construct a risk model, all genes from TCGA and GSE39582 datasets were extracted and used to generate a prognostic gene signature. These genes were then subjected to univariate Cox regression and KM analyses. In TCGA and GSE39582 datasets, 113 genes are

significantly associated with prognosis in patients with CRC (Fig. 1A). These overlapping genes were then used for the LASSO regression analysis to avoid overfitting problems in the risk signature. The AIC method of the multivariate Cox regression analysis was applied to the genes returned from the LASSO regression analysis to construct the optimal model, which included 15 genes (GSTM1, PCDHB2, DAPK1, TTC12, EXOC3L4, CCL22, TERF2IP, TLE6, NUMBL, ZNF180, LINC00261, ERFE, CDCA2, LINC00638 and GPRASP1) (Fig. 1B and C). Among these genes, TTC12, CCL22, ZNF180, LINC00261 and CDCA2 were revealed to be protective factors with HRs <1, whereas GSTM1, PCDHB2, DAPK1, EXOC3L4, TERF2IP, TLE6, NUMBL, ERFE, LINC00638 and GPRASP1 were considered risk factors with HRs >1 (Fig. 1H). TCGA dataset was used as a training cohort to construct the risk signature. Samples in TCGA and GSE39582 cohorts were stratified into low- and

high-risk groups based on the median risk score in each cohort. The KM analysis showed that patients in the low-risk group were associated with better outcomes than those in the high-risk group (Fig. 1D and E). All 15 genes exhibited significant differences in gene expression between the low- and high-risk groups (Fig. 1F); 10 genes were upregulated in the high-risk group and five genes were upregulated in the low-risk group. In addition, most of them exhibited differential expression between tumor and adjacent normal tissues in TCGA dataset (Fig. S1A). The OS-related prediction model distribution of patients in TCGA and GSE39582 datasets is shown in Fig. 1G.

ZNF180 is dysregulated in CRC cell lines and tissues. Among the 15 genes identified, only ZNF180 encoded a transcription factor. Transcription factors are potential regulatory genes and mediators of tumor progression (30,31). Notably, the function and mechanisms of ZNF180 in CRC are poorly understood; therefore, ZNF180 was selected for further functional and downstream target exploration, aiming to elucidate its clinical characteristics and prognostic value in CRC. To investigate the role of ZNF180 in CRC progression, its expression was assessed in CRC cells and tissues. The results revealed that the mRNA expression levels of ZNF180 were decreased in most CRC cell lines compared with those in HIEC-6 immortalized intestinal epithelial cells (Fig. 2A). In addition, ZNF180 mRNA and protein expression levels were detected in CRC patient tissue samples and matched normal tissues by RT-qPCR and western blotting. The relative expression levels of ZNF180 were significantly lower in 12 CRC tissues than those in 12 normal tissues from the SYSU6 cohort (Figs. 2C-E and S1F); these results were consistent with those recorded from TCGA and GSE39582 datasets (Fig. S1B). The mRNA expression levels of ZNF180 in numerous CRC cell lines were obtained from the DepMap portal (Fig. S3A).

Based on these findings, it was hypothesized that ZNF180 may serve a crucial role in CRC tumorigenesis. The clinical implications of ZNF180 expression were further evaluated using IHC staining in 220 CRC samples from the SYSU6 cohort (Fig. 2F). Based on the ROC curve, the optimal cut-off of ZNF180 expression was identified and patients were divided into low- and high ZNF180 expression groups. The KM analysis showed that patients with high ZNF180 expression had a longer OS and DFS than those with low ZNF180 expression in the SYSU6 cohort (Figs. 2H and S1C); this was also observed in TCGA and GSE39582 datasets (Fig. S1D). ZNF180 expression was slightly associated with the risk score in both TCGA and GSE39582 datasets (Fig. S1E). Notably, there was a high proportion of high ZNF180 expression in normal tissues (Fig. 2G). The associations between ZNF180 expression and clinicopathological characteristics of 220 patients with CRC in the SYSU6 cohort are presented in Table I. Low levels of ZNF180 in primary tumors were significantly associated with advanced T, N, M and clinical stages, and a high risk of mortality and disease progression. Collectively, these results indicated a strong association between ZNF180 expression and patient survival outcomes, suggesting a critical role of ZNF180 in CRC pathogenesis.

ZNF180 is downregulated and regulated by methylation in CRC. Aberrant DNA methylation is one of the most common defects in epigenetic regulation observed in tumorigenesis (12,32), and DNA methylation can decrease gene expression. As aforementioned, ZNF180 expression was significantly decreased in tumor tissues compared with in adjacent normal tissues (Fig. 2C and D); therefore, the present study investigated whether the downregulation of ZNF180 expression was regulated by methylation in CRC. The CpG islands in the ZNF180 promoter region are shown in Fig. 3A. Initially, CRC cells were treated with 5-AzaC, a DNMT inhibitor. The results revealed that treatment with 5-AzaC significantly increased the mRNA and protein expression levels of ZNF180 in CRC cells (Fig. 3B and C). In addition, ZNF180 methylation was slightly associated with ZNF180 mRNA expression in TCGA dataset (Fig. 3D). The KM analysis showed that patients with low ZNF180 methylation levels had a longer OS than those with high ZNF180 methylation levels in TCGA dataset (Fig. 3E). Moreover, the expression of ZNF180 was also associated with genomic alteration (Fig. 3F). In summary, it may be hypothesized that the expression of ZNF180 is regulated by methylation and genomic alteration. To examine the role of ZNF180 in CRC progression, ZNF180-overexpressing HCT116 and RKO stable cell lines were established. ZNF180 mRNA and protein expression levels were verified by RT-qPCR and western blotting, respectively (Fig. 3G and H). The effect of ZNF180 overexpression on HCT15 cells was poor at the protein level, and since the function of genes mainly depends on protein levels, the two other cell lines (HCT116 and RKO) that exhibited overexpression at the protein level were selected for the subsequent functional study.

ZNF180 overexpression inhibits CRC cell proliferation and induces apoptosis. To examine the effect of ZNF180 on apoptosis, flow cytometry and western blotting were performed. Annexin V and PI staining indicated that 5-FU induced more apoptosis in the ZNF180-overexpressing HCT116 and RKO cells than in the vector-transduced cells in a dose-dependent manner (Fig. 4A and B). This indicated that the ZNF180-overexpressing cell line was more sensitive to 5-FU than the control cell line. Moreover, the expression levels of cleaved-PARP were increased in ZNF180-overexpressing cells upon treatment with 5-FU, whereas the expression levels of PARP were lower, compared with those in the vector-transduced cells (Fig. 4C). These data suggested that ZNF180 may confer sensitivity to 5-FU. EdU staining was also performed to assess the effects of ZNF180 on proliferation. The results showed that ZNF180-overexpressing cells exhibited less EdU staining than vector-transduced cells (Fig. S2C and D). The results of IF staining showed that Ki67 expression was also decreased in ZNF180-overexpressing cells (Fig. S2E-G).

Subsequently, an animal xenograft model was prepared by subcutaneously injecting cells with stable overexpression of ZNF180 and vector-transduced cells into nude mice. The ZNF180-overexpressing group presented decreased tumor growth compared with the vector group (Fig. 4E). Images of the isolated tumors are shown in Fig. 4D. Additionally, when 2×10^6 cells were injected into nude mice, 75% of the mice (9/12) formed palpable tumors in the HCT116 vector group compared with

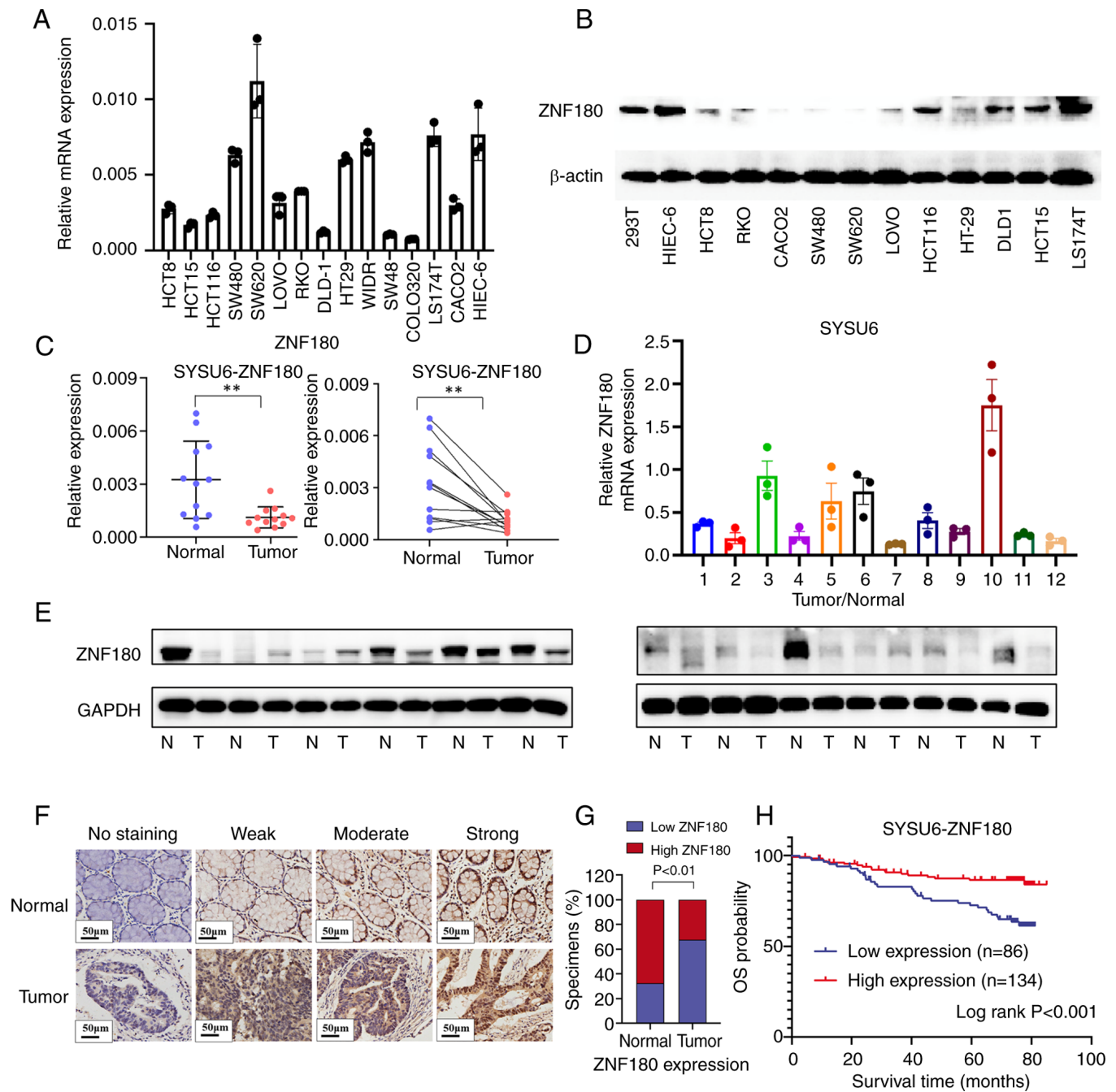


Figure 2. ZNF180 expression is frequently downregulated in CRC tissues and cell lines. (A) mRNA expression levels of ZNF180 in CRC cell lines and HIEC-6 immortalized intestinal epithelial cells. (B) Protein expression levels of ZNF180 in CRC cell lines and HIEC-6 immortalized intestinal epithelial cells. (C) mRNA expression levels of ZNF180 in 12 paired CRC tissues and adjacent normal tissues from the SYSU6 cohort were confirmed by reverse transcription-quantitative PCR. **P<0.01. (D) Relative expression of ZNF180 in tumors was compared with the relative expression of ZNF180 in adjacent normal tissues. (E) Protein expression levels of ZNF180 in 12 paired CRC tissues and adjacent normal tissues from the SYSU6 cohort were confirmed by western blotting. (F) Levels of ZNF180 protein expression in CRC tissues were detected under high magnification microscopy. (G) Low ZNF180 expression rate was higher in CRC tissues; tissues from 40 patients in the SYSU6 cohort with both normal and tumor cells were assessed. (H) OS rate of patients in the SYSU6 cohort (n=220) was significantly higher in the high ZNF180 expression group. CRC, colorectal cancer; N, normal; OS, overall survival; SYSU6, The Sixth Affiliated Hospital of Sun Yat-sen University; T, tumor; ZNF180, zinc finger protein 180.

50% of the mice (6/12) in the HCT116 ZNF180-overexpressing group on day 5 (Fig. 4F). There was no difference in the body weight of mice between the ZNF180-overexpressing group and vector group (Fig. 4G). In addition, the expression of ZNF180 and METTL14 were assessed using IHC staining in tumor tissues obtained from the mice (Fig. 4H). In the ZNF180-overexpression group, higher expression of ZNF180 and METTL14 was detected in mouse tumor tissues.

To investigate the possible mechanism underlying the inhibitory effects of ZNF180 on cell proliferation, the cell cycle progression of ZNF180-overexpressing and vector-transduced cells was assessed. The results showed that ZNF180 did not exert an effect on cell cycle progression (Fig. S2H). To investigate the biological function of ZNF180 in CRC, wound healing and Transwell assays were carried out. The experiments demonstrated that ZNF180 did not have an effect on

Table I. Association of ZNF180 expression and clinical characteristics in 220 patients with colorectal cancer from The Sixth Affiliated Hospital of Sun Yat-sen University cohort.

Characteristic	No.	ZNF180 expression		P-value
		Low	High	
Sex				0.401
Male	130	54	76	
Female	90	32	58	
Age				0.052
≤60 years	128	43	85	
>60 years	92	43	49	
OS				0.0001 ^a
No	172	56	116	
Yes	48	30	18	
DFS				0.012 ^a
No	150	50	100	
Yes	70	36	34	
Location				0.624
Right	51	18	33	
Left	169	68	101	
T stage				0.003 ^a
I-II	61	14	47	
III-IV	159	72	87	
N stage				0.005 ^a
N ₀	144	45	99	
N _{1-X}	76	41	35	
M stage				0.001 ^a
M ₀	190	66	124	
M ₁	30	20	10	
Clinical stage				0.0001 ^a
I-II	135	40	95	
III-IV	85	46	39	

^aP<0.05. DFS, disease-free survival; OS, overall survival; ZNF180, zinc finger protein 180.

migration and invasion (Fig. S2I and J). These results revealed the critical role of ZNF180 in inhibiting cell proliferation and inducing apoptosis.

METTL14 is a candidate downstream molecule in ZNF180 signaling. Transcription factors can finely regulate the expression of downstream genes at specific developmental stages by directly binding gene promoters and enhancers, or changing chromatin structure (33,34). Currently, the function of ZNF180 in CRC, particularly in the regulation of downstream genes, is poorly characterized. To identify the potential target genes of ZNF180 in CRC, 478 genes that were significantly co-expressed with ZNF180 were selected by overlapping three different cohorts, namely TCGA, GSE39582 and GSE87211 (Fig. 5A and B). In the correlation analysis, the correlation coefficient between METTL14

and ZNF180 was ranked in the top 10. Moreover, previous literature has reported that METTL14 is a tumor suppressor gene (18-20), and that METTL14 expression in primary CRC may be an independent favorable prognostic factor for OS in patients (35).

Based on the aforementioned analysis, METTL14 may be considered a candidate target for the ZNF180 gene. Considering that ZNF180 was regulated by methylation in CRC, the present study mainly focused on the candidate genes relevant to DNA methylation. According to previous literature, METTL14 is a well-established m⁶A writer protein and m⁶A methylation can be catalyzed by METTL14 (16). To examine the role of METTL14 in CRC progression, its expression was assessed in CRC cells and tissues. It was observed that the mRNA and protein expression levels of METTL14 were decreased in most CRC cell lines compared with those in HIEC-6 immortalized intestinal epithelial cells (Figs. 5C and D). The mRNA expression levels of METTL14 in numerous CRC cell lines were obtained from DepMap portal (Fig. S3B). In addition, the mRNA and protein expression levels of METTL14 were detected in 12 CRC tissue samples and matched normal tissues by RT-qPCR and western blotting (Figs. 5E and F, and S1G). The relative expression levels of METTL14 were significantly lower in CRC tissues than in normal colorectal tissues in the SYSU6, TCGA, GSE39582 and GSE87211 cohorts (Figs. 5G and S2A). These findings indicated that ZNF180 expression was closely associated with the candidate gene METTL14 expression.

METTL14 is positively correlated with ZNF180 expression in CRC cell lines and tissues. To examine the role of METTL14 in CRC progression, its expression was assessed in CRC cells and tissues. The mRNA and protein expression levels of METTL14 were detected in 12 CRC tissue samples and 12 non-cancerous colorectal tissues by RT-qPCR in the SYSU6 cohort (Figs. 5G and 6A). The relative expression levels of METTL14 were significantly lower in CRC tissues than in normal colorectal tissues in the SYSU6 cohort (Fig. 5G); ZNF180 expression was positively correlated with METTL14 expression in CRC cell lines, and tissues in the SYSU6, TCGA and GEO cohorts (Fig. 6A-E). The KM analysis showed that patients with high METTL14 expression had better outcomes than those with low METTL14 expression in TCGA dataset (Fig. 6F). The result was consistent with previously reported data (36). The clinical implications of METTL14 expression were further assessed using IHC staining of 40 pairs of CRC samples. The relative protein levels of METTL14 were markedly decreased in CRC tissues compared with in normal colorectal tissues by IHC staining (Fig. 6G); there was a high proportion of high METTL14 expression in normal tissues, and a high proportion for high METTL14 expression in high ZNF180-expressing tissues (Fig. 6H). Collectively, these results indicated a positive correlation between METTL14 and ZNF180 expression levels.

ZNF180 directly binds to and promotes METTL14 in CRC. The increase in METTL14 expression at the mRNA and protein levels after the overexpression of ZNF180 was validated by RT-qPCR and western blotting, respectively (Fig. 7A and C). The IF assay showed that ZNF180 and

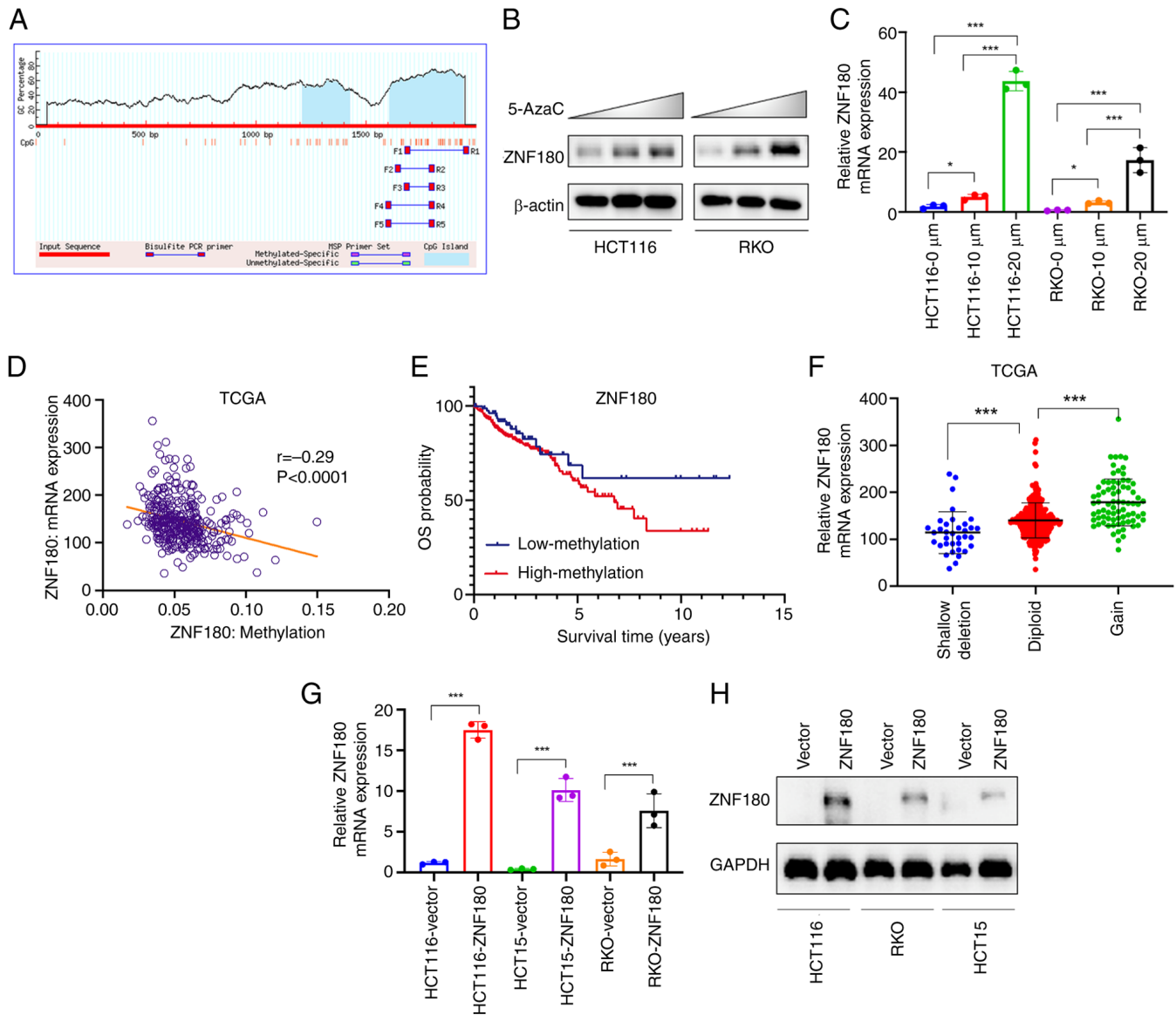


Figure 3. ZNF180 is downregulated and its promoter hypermethylated in colorectal cancer. (A) Schematic representation of the CpG islands and bisulfite sequencing region in the ZNF180 promoter. HCT116 and RKO cells were subjected to 3 days of treatment with increasing doses of 5-AzaC; blue: CpG island of ZNF180 promoter; Input Sequence: Promoter region of ZNF180. (B) Protein expression levels were determined by western blotting. (C) mRNA expression levels were determined by RT-qPCR, respectively. The untreated group was used as the control group, and the relative expression levels of each group were divided by the relative expression levels of the control group. P-values were calculated using one-way ANOVA and Scheffe test, $^*P < 0.05$, $^{***}P < 0.001$. (D) Correlation between ZNF180 mRNA expression level and ZNF180 methylation level in TCGA data set. (E) Overall survival rate was significantly higher in the low ZNF180 methylation group in TCGA dataset. (F) ZNF180 mRNA expression in patients with different DNA statuses in TCGA dataset. P-values were calculated using one-way ANOVA and Scheffe test, $^{***}P < 0.001$. Relative (G) mRNA and (H) protein expression levels were determined by RT-qPCR and immunoblotting, respectively. P-values were calculated using unpaired Student's t-test, $^{***}P < 0.001$. 5-AzaC, 5-azacytidine; RT-qPCR, reverse transcription-quantitative PCR; TCGA, The Cancer Genome Atlas; ZNF180, zinc finger protein 180.

METTL14 were mainly located in the nucleus, and that the overexpression of ZNF180 increased METTL14 expression (Figs. 7B and S2K). Since ZNF180 is a transcription factor, it was hypothesized that the METTL14 promoter could be regulated by ZNF180. For the mechanistic analysis, a ChIP assay was performed. ZNF180 was detected in cell lines stably overexpressing ZNF180 by blotting using a specific anti-Flag antibody. Using the ChIP assay, DNA was digested into 100-750 bp fragments (Fig. 7D), and the ZNF180 protein was successfully pulled down with an anti-Flag antibody. A METTL14 DNA element was detected in the anti-Flag group (Fig. 7E). Based on the METTL14 promoter regions

(Table SI), specific primers were designed for standard PCR assay, and the METTL14 levels were also detected by RT-qPCR and normalized to those of IgG (Fig. 7F), thus indicating that METTL14 may be a downstream target gene of ZNF180. To verify whether ZNF180 can bind to the METTL14 promoter, the METTL14 promoter (2,030 bp) was cloned into a luciferase plasmid. The luciferase assay results showed that the transcriptional activity was increased in the METTL14 promoter plasmid group compared with the vector group (Fig. 7G). This finding showed that the region of the METTL14 promoter was transcriptionally activated by ZNF180. Furthermore, METTL14 was knocked

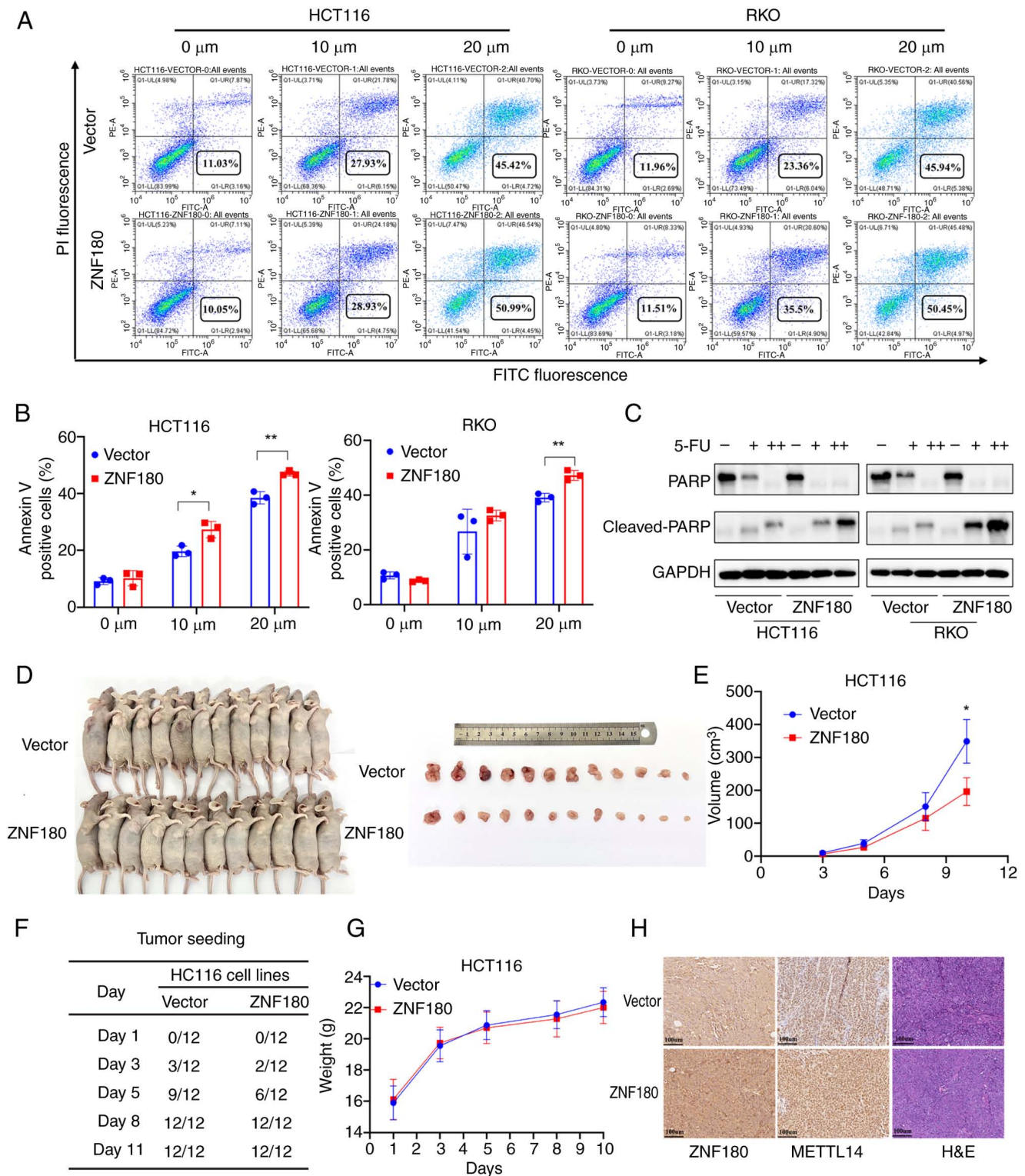


Figure 4. ZNF180 enhances cellular sensitivity and suppresses cell growth *in vivo*. (A) Cells were double-stained with PI and Annexin V, and analyzed by flow cytometry to evaluate apoptosis. (B) Quantification of the percentage of apoptotic cells. P-values were calculated using unpaired Student's t-test. * $P < 0.05$, ** $P < 0.01$. (C) HCT116 vector cells and HCT116 ZNF180-overexpressing cells were treated with increasing doses of 5-FU for 48 h, and PARP and cleaved-PARP expression was analyzed by western blotting. GAPDH was used as the loading control. (D) HCT116 cells expressing the control vector or overexpressing ZNF180 were subcutaneously inoculated into nude mice. Images of isolated tumors are shown. (E) Growth curve indicates HCT116 growth suppression upon ZNF180 overexpression compared with vector *in vivo*. P-values were calculated using unpaired Student's t-test, * $P < 0.05$ vs. ZNF180. (F) HCT116 (2×10^6) cells were subcutaneously injected into nude mice and were monitored every 2 days. (G) Weight of nude mice during tumorigenesis. (H) Representative immunohistochemistry and H&E staining images of ZNF180 and METTL14 expression in mice tumor tissues. 5-FU, 5-fluorouracil; H&E, hematoxylin and eosin; METTL14, methyltransferase 14, N6-adenosine-methyltransferase non-catalytic subunit; ZNF180, zinc finger protein 180.

down using siRNA and validated by western blot (Fig. 7H); the proliferation assay results showed that knockdown of

METTL14 promoted tumor cell proliferation (Fig. 7I), and knockdown of METTL14 could reverse the inhibition of cell

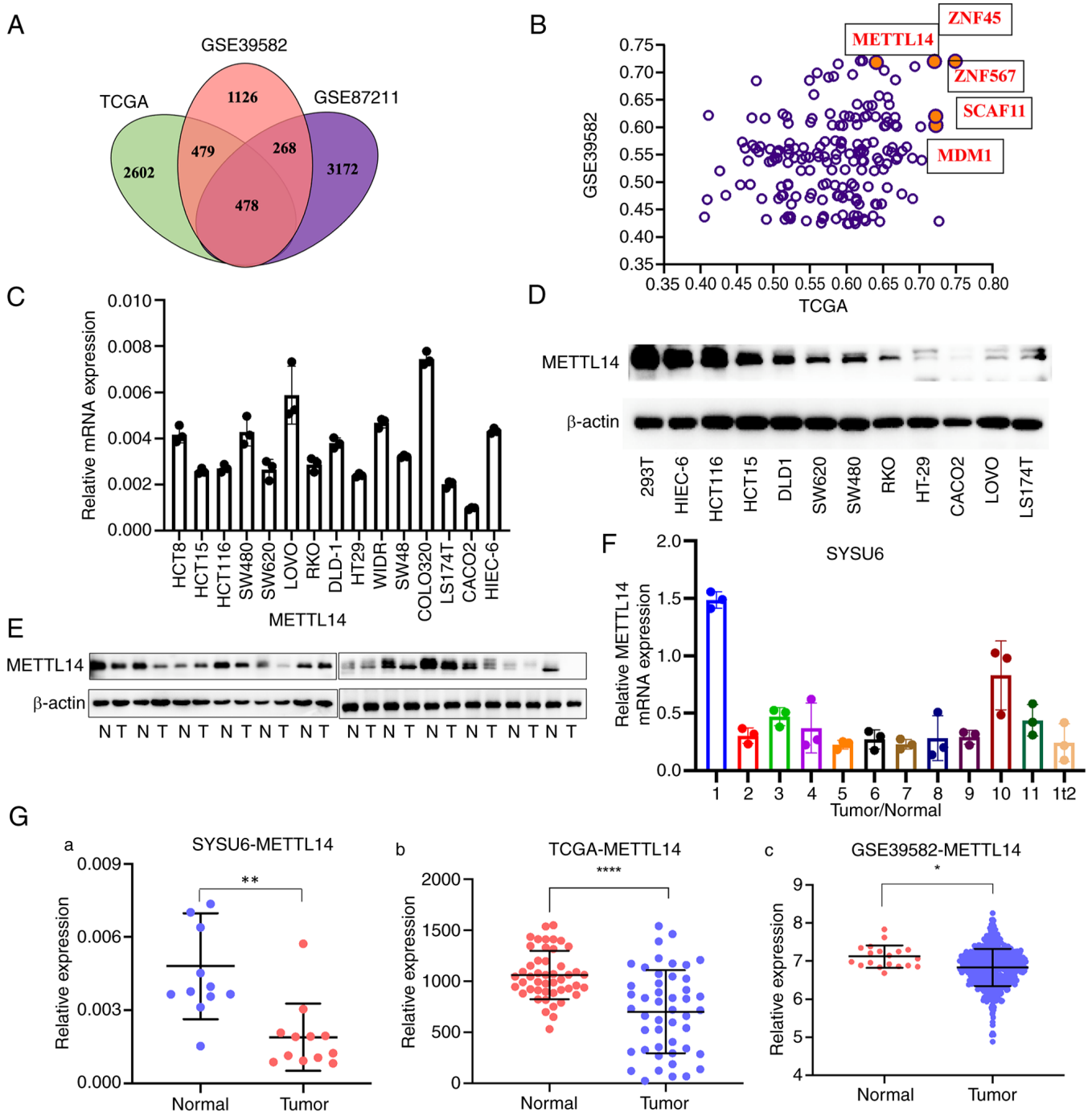


Figure 5. METTL14 is a candidate target gene of ZNF180. (A) Overlapping of the differentially expressed genes from TCGA, GSE39582 and GSE87211 cohorts; 478 genes were identified to be correlated with ZNF180. (B) Correlation between candidate target genes and ZNF180 in TCGA and GSE39582 cohorts. (C) mRNA expression levels of METTL14 in CRC cell lines and HIEC-6 immortalized intestinal epithelial cells. (D) Protein expression level of METTL14 in CRC cell lines and HIEC-6 immortalized intestinal epithelial cells. (E) Protein and (F) mRNA expression levels of METTL14 in 12 paired CRC tissues and noncancerous tissues from the SYSU6 cohort were confirmed by western blotting and reverse transcription-quantitative PCR, respectively. (G) mRNA expression levels of METTL14 in CRC tissues and noncancerous tissues in SYSU6 (12 pairs), TCGA (47 pairs) and GSE39582 (normal tissues=19, tumor tissues=566) cohorts. P-values were calculated using paired Student's t-test (a and b) or unpaired Student's t-test (c). * $P < 0.05$, ** $P < 0.01$, **** $P < 0.0001$. CRC, colorectal cancer; METTL14, methyltransferase 14, N6-adenosine-methyltransferase non-catalytic subunit; N, normal; SYSU6, The Sixth Affiliated Hospital of Sun Yat-sen University; T, tumor; TCGA, The Cancer Genome Atlas; ZNF180, zinc finger protein 180.

proliferation by ZNF180 (Fig. S1H). To demonstrate whether METTL14 can rescue the effect of ZNF180 by increasing apoptosis, cell lines with stable overexpression of ZNF180 and METTL14 knockdown were constructed using siRNA in ZNF180-overexpressing HCT116 cell lines. Following treatment with 5-FU, flow cytometry was performed to

determine the effects of METTL14 on cancer cell apoptosis (Fig. 7J and K); the results revealed that knockdown of METTL14 could rescue the effects of ZNF180 on apoptosis. These results indicated that ZNF180 directly binds to the METTL14 DNA element and activates the transcriptional activity of the METTL14 gene (Fig. 8).

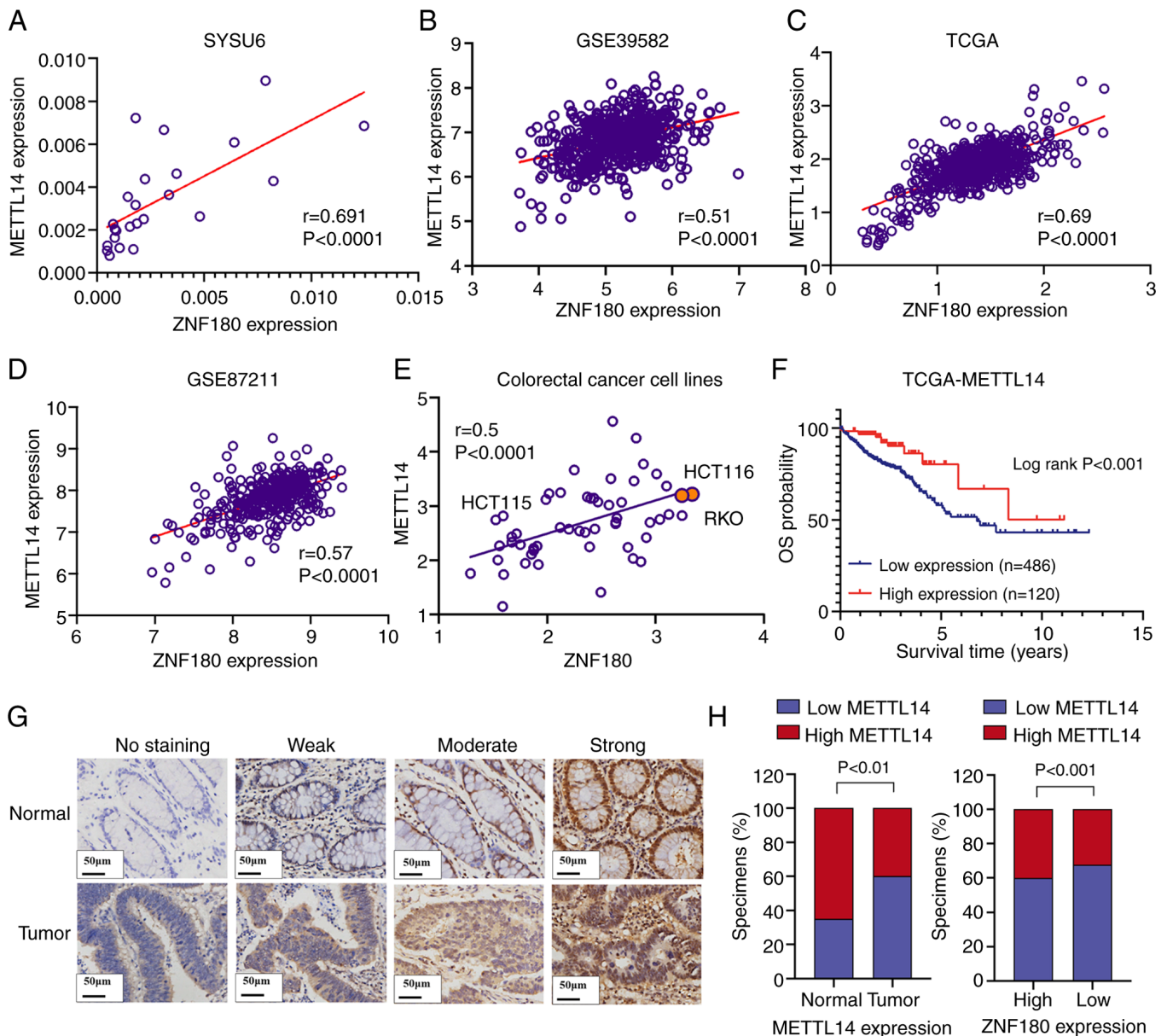


Figure 6. METTL14 is associated with ZNF180 in CRC cell lines and tissues. (A) mRNA expression levels of METTL14 in 12 paired CRC tissues and noncancerous tissues from the SYSU6 cohort, and the positive correlation between METTL14 and ZNF180 expression in the SYSU6 cohort. Pearson correlation coefficient was used for correlation analyses. $^{**}P<0.01$. (B) ZNF180 expression was positively correlated with METTL14 expression in the GSE39582 dataset. (C) mRNA expression levels of ZNF180 and METTL14 in CRC tissues, the positive correlation between METTL14 and ZNF180 expression in TCGA dataset. Pearson correlation coefficient was used for correlation analyses. $^{****}P<0.0001$. (D) ZNF180 expression was positively correlated with METTL14 expression in the GSE87211 data set. (E) Positive correlation between METTL14 and ZNF180 expression in CRC cell lines. Pearson correlation coefficient was used for correlation analyses. $^{****}P<0.0001$. (F) Kaplan-Meier analysis indicated downregulation of METTL14 was significantly associated with poorer overall survival in patients with CRC in TCGA dataset. (G) Levels of METTL14 protein expression in CRC tissues under high magnifications microscopy. (H) Low METTL14 expression rate was higher in CRC tissues, and the high METTL14 expression rate was increased in the high ZNF180 expression group; tissues from 40 patients with CRC in the SYSU6 cohort with both tumor cells and normal cells were assessed. CRC, colorectal cancer; METTL14, methyltransferase 14, N6-adenosine-methyltransferase non-catalytic subunit; SYSU6, The Sixth Affiliated Hospital, Sun Yat-sen University; TCGA, The Cancer Genome Atlas; ZNF180, zinc finger protein 180.

Discussion

CRC is a disorder caused by the progressive accumulation of genetic and epigenetic alterations that may promote dysplasia and tumorigenesis (37,38). The popularity of next-generation sequencing has facilitated the production of large amounts of data for the construction of multi-gene profiles, which can help stratify risk and guide chemotherapy for various types of cancer (39-41). Artificial intelligence

and bioinformatics can uncover differentially expressed and survival-associated genes with potential prognostic and treatment-related properties. Therefore, investigating the dysregulated genes involved in carcinogenesis and disease development may improve the prognosis and treatment of patients with CRC.

Gene expression is regulated by a combination of numerous *cis*-regulatory elements, including core promoters and promoter-proximal elements, as well as various *cis*-regulatory

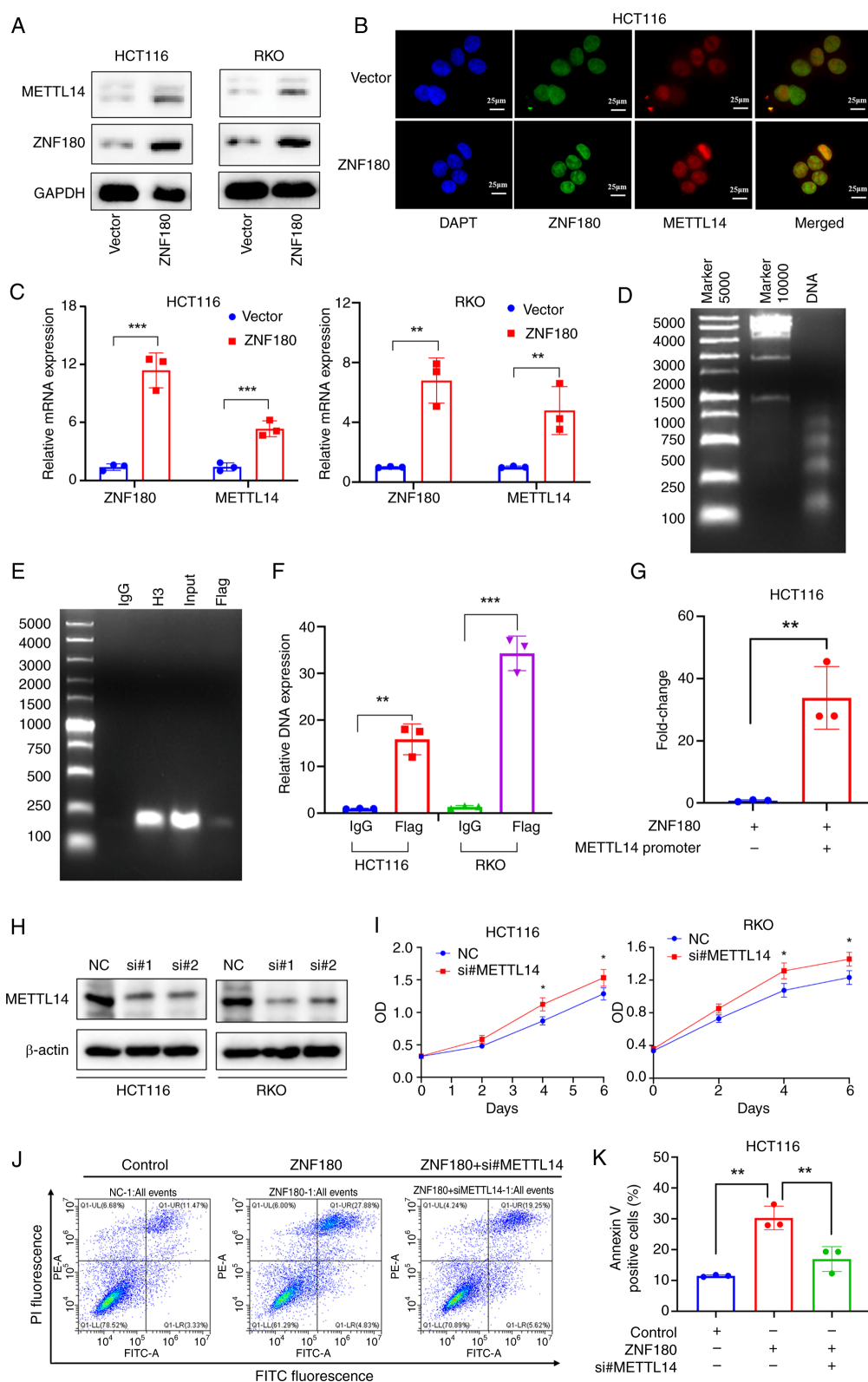


Figure 7. METTL14 is a candidate downstream molecule in ZNF180 signaling. (A) ZNF180 and METTL14 expression were measured by western blotting. (B) Localization of ZNF180 and METTL14 in HCT116 cells by confocal immunofluorescence analysis. (C) Overexpression of ZNF180 in HCT116 and RKO cells; ZNF180 and METTL14 mRNA expression levels were detected by RT-qPCR. P-values were calculated using unpaired Student's t-test, ** $P < 0.01$, *** $P < 0.001$. (D) Agarose gel electrophoresis showed that DNA was digested into 100-750 bp. (E) Cells stably transfected with vector or flag-ZNF180 were analyzed by ChIP, and METTL14 DNA was qualitatively analyzed using DNA agarose gel electrophoresis. IgG refers to normal rabbit IgG (negative control) and H3 refers to histone H3 (positive control). (F) METTL14 DNA element was quantified by RT-qPCR. P-values were calculated using unpaired Student's t-test, ** $P < 0.01$, *** $P < 0.001$. (G) METTL14-luciferase activity in 293T cells overexpressing ZNF180. P-values were calculated using unpaired Student's t-test, ** $P < 0.01$. (H) Protein expression levels of METTL14 were determined by immunoblotting. (I) Cell proliferation was determined using the MTS assay. P-values were calculated using unpaired Student's t-test, * $P < 0.05$ vs. NC. (J) Cells were double-stained with PI and Annexin V, and analyzed by flow cytometry to evaluate apoptosis. (K) Quantification of the percentage of apoptotic cells. P-values were calculated using one-way ANOVA (parametric) test and Scheffe test, ** $P < 0.01$. METTL14, methyltransferase 14, N6-adenosine-methyltransferase non-catalytic subunit; NC, negative control; OD, optical density; RT-qPCR, reverse transcription-quantitative PCR; si, small interfering; ZNF180, zinc finger protein 180.

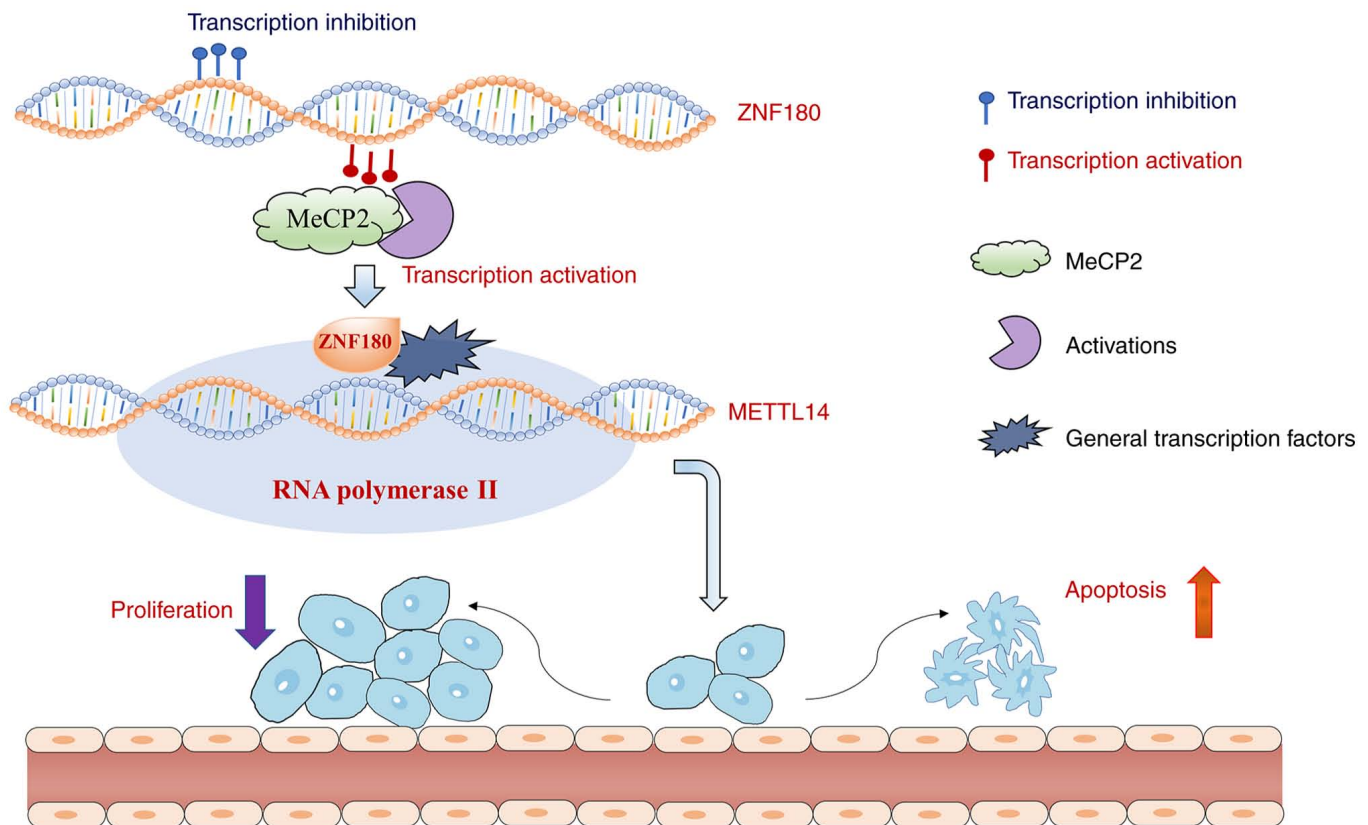


Figure 8. Mechanism of how ZNF180 induces an apoptotic phenotype by activating METTL14 transcriptional activity in colorectal cancer. METTL14, methyltransferase 14, N6-adenosine-methyltransferase non-catalytic subunit; ZNF180, zinc finger protein 180.

modules located distant from the transcription start sites, such as enhancers (42,43), silencers (44-46), insulators (47) and tethering elements (48,49). Among these elements, enhancers and their associated transcription factors serve a leading role in the initiation of gene expression. The identification of enhancer and promoter positions has been the focus of several studies (50,51).

The present study performed transcriptome analysis and obtained relevant clinicopathological data from 606 and 505 patients with CRC from TCGA and GSE39582 cohorts, respectively. A novel prognostic model was generated based on a gene expression signature classifier to predict the OS of patients with CRC. LASSO regression analysis was used to construct the optimal model, which included 15 genes (GSTM1, PCDHB2, DAPK1, TTC12, EXOC3L4, CCL22, TERF2IP, TLE6, NUMBL, ZNF180, LINC00261, ERFE, CDCA2, LINC00638 and GPRASP1), and developed a prognostic model that stratified patients into low- and high-risk groups. This model was validated in TCGA and GSE39582 cohorts. Transcription factors are potential regulatory genes and mediators of tumor progression, and the functions and mechanisms of ZNF180 in CRC are poorly understood. Thus, ZNF180 was selected for further functional and downstream target exploration, aiming to elucidate its clinical characteristics and prognostic value in CRC.

The present study first demonstrated that the expression of ZNF180 was regulated by methylation. Moreover, it was determined that ZNF180 was a prognostic protective factor for CRC based on gene expression data. To examine the role of ZNF180

in CRC progression, ZNF180-overexpressing HCT116 and RKO stable cell lines were established. The functional assays revealed that elevated ZNF180 expression suppressed cell proliferation, induced a higher rate of apoptosis, and enhanced cell chemotherapeutic sensitivity by treatment with 5-FU compared with a vector. Taken together, these data revealed the critical role of ZNF180 in inhibiting proliferation and inducing apoptosis.

ZNF180 is a member of the ZNF family of transcription factors (52). Transcription factors serve vital roles in regulating tumorigenesis, and individual transcription factors may have different or even opposite functions among various cancer types (36,53). Thus, a suitable tool was necessary to elucidate the role of ZNF180 in the tumorigenesis of CRC. Based on the ChIP assay and clinical correlation analysis, the present study identified METTL14, which is a major RNA N6-adenosine methyltransferase, as a candidate downstream target of ZNF180.

Subsequently, the present study focused on METTL14 for further analysis, and it was revealed to be located in the nucleoplasm. Its principal function is to enable mRNA binding activity, and it contributes to mRNA (2'-O-methyladenosine-N6-)-methyltransferase activity (54,55). It is also involved in the mRNA metabolic process, and regulation of hematopoietic progenitor cell differentiation and positive regulation of translation (19,56). To identify the potential target genes of ZNF180 in CRC, 478 genes significantly co-expressed with ZNF180 were selected by overlapping three different cohorts. In the correlation

analysis, the correlation coefficient between METTL14 and ZNF180 was ranked in the top 10. By conducting a series of experiments, a positive correlation was identified between ZNF180 and METTL14 expression at the mRNA and protein levels, and ZNF180 overexpression was shown to increase METTL14 expression in CRC cell lines. Further investigation suggested that METTL14 was a potential downstream target gene of ZNF180 in CRC and may be a prognostic protective factor in CRC. Previous research has shown that METTL14 expression in primary CRC may be an independent favorable prognostic factor for OS in patients (35). Moreover, the evidence showed that METTL14 suppresses proliferation in CRC. This finding is consistent with the data obtained for ZNF180 signaling in the present study. METTL14 is a key protein in the m⁶A pathway, and its role in CRC has been reported by Chen *et al* (18); METTL14 has been shown to inhibit CRC cell migration, invasion and metastasis, and to epigenetically inhibit the expression of SOX4 via an m⁶A-YTHDF2-dependent mechanism in CRC. METTL14 has also been demonstrated to participate in promoting cardiovascular endothelial cell proliferation and invasion (17).

To the best of our knowledge, the present study is the first to evaluate the critical roles of ZNF180 in inhibiting CRC proliferation and inducing apoptosis. The results demonstrated that ZNF180 may have a crucial role in CRC tumorigenesis, and that ZNF180 is regulated by methylation. In addition, ZNF180 and METTL14 genes were identified as prognostic protective factors in CRC. Moreover, a close relationship between ZNF180 and METTL14 expression was revealed in cell lines, tissues and different cohorts. The present findings confirmed that ZNF180 is a tumor suppressor gene that may directly bind to the upstream region of METTL14 and activate its expression in CRC cells.

In summary, the findings of the present study reveal a fundamental relationship between ZNF180 and METTL14. ZNF180 was shown to be downregulated by methylation, and to upregulate METTL14 by binding directly to METTL14 DNA elements, thereby inhibiting cell proliferation and inducing apoptosis. The present results suggested that ZNF180 directly interacts with and activates METTL14 transcriptional activity and positively regulates its expression. The ZNF180/METTL14 axis may be a prognostic biomarker and effective therapeutic target for CRC.

Acknowledgements

The authors would like to thank Mr. Minzhi Qiu for his contributions to the adjustment of the figures.

Funding

This work was supported by grants from the National Key R&D Program of China (grant no. 2022YFA1304000), the National Natural Youth Science Foundation of China (grant no. 32000555), the Guangzhou Basic and Applied Basic Research Project (grant no. SL2022A04J01659), the program of Guangdong Provincial Clinical Research Center for Digestive Diseases (grant no. 2020B1111170004) and the National Key Clinical Discipline.

Availability of data and materials

The data generated in the present study may be requested from the corresponding author.

Authors' contributions

QY and LX wrote the original draft. YH, PL, LSZ, LX, XJC, HLL, XTL, JPX, WTS, JLH, ZTC, XLT, HJL and XHF wrote, reviewed and edited the manuscript. YH, PL, QY, LX, LSZ, JPX, and XJC performed the conceptualization. XJC, HLL, XTL, XLT, HJL, and ZTC performed the data analysis. LX, XTL, XHF and JLH performed the formal analysis. YH, PL, QY, LSZ and LX provided the funding. YH, QY, LX, HLL and WTS designed the methodology, created the animal models and performed some experiments. XTL and JLH performed the project administration. LSZ, LX, XJC, XLT, XTL and JPX provided study materials and reagents. PL, QY and LSZ performed the supervision. LX and HJL performed the validation. HLL and JPX generated the figures. LX and YH confirm the authenticity of all the raw data. All authors read and approved the final version of the manuscript.

Ethics approval and consent to participate

The present study involving human samples was approved by the Institutional Review Board of SYSU6 (approval no. 2021ZSLYEC-228), and all patients provided written informed consent for their tissues to be used in medical research. The animal experiment was approved by the Investigation Ethical Committee of The Sixth Affiliated Hospital of Sun Yat-sen University (approval no. IACUC-2023101301).

Patient consent for publication

Not applicable.

Competing interests

The authors declare that they have no competing interests.

References

1. Siegel RL, Miller KD, Fuchs HE and Jemal A: Cancer Statistics, 2021. *CA Cancer J Clin* 71: 7-33, 2021.
2. Siegel RL, Wagle NS, Cercek A, Smith RA and Jemal A: Colorectal cancer statistics, 2023. *CA Cancer J Clin* 73: 233-254, 2023.
3. Roth AD, Tejjap S, Delorenzi M, Yan P, Fiocca R, Klingbiel D, Dietrich D, Biesmans B, Bodoky G, Barone C, *et al*: Prognostic role of KRAS and BRAF in stage II and III resected colon cancer: Results of the translational study on the PETACC-3, EORTC 40993, SAKK 60-00 trial. *J Clin Oncol* 28: 466-474, 2010.
4. Xu RH, Muro K, Morita S, Iwasa S, Han SW, Wang W, Kotaka M, Nakamura M, Ahn JB, Deng YH, *et al*: Modified XELIRI (capecitabine plus irinotecan) versus FOLFIRI (leucovorin, fluorouracil, and irinotecan), both either with or without bevacizumab, as second-line therapy for metastatic colorectal cancer (AXEPT): A multicentre, open-label, randomised, non-inferiority, phase 3 trial. *Lancet Oncol* 19: 660-671, 2018.
5. Xie Y, Shi L, He X and Luo Y: Gastrointestinal cancers in China, the USA, and Europe. *Gastroenterol Rep (Oxf)* 9: 91-104, 2021.
6. Okada M, Wang CY, Hwang DW, Sakaguchi T, Olson KE, Yoshikawa Y, Minamoto K, Mazer SP, Yan SF and Pinsky DJ: Transcriptional control of cardiac allograft vasculopathy by early growth response gene-1 (Egr-1). *Circ Res* 91: 135-142, 2002.

7. Song WM, Agrawal P, Von Itter R, Fontanals-Cirera B, Wang M, Zhou X, Mahal LK, Hernando E and Zhang B: Network models of primary melanoma microenvironments identify key melanoma regulators underlying prognosis. *Nat Commun* 12: 1214, 2021.
8. Klutstein M, Nejman D, Greenfield R and Cedar H: DNA methylation in cancer and aging. *Cancer Res* 76: 3446-3450, 2016.
9. El Helou R, Wicinski J, Guille A, Adélaïde J, Finetti P, Bertucci F, Chaffanet M, Birnbaum D, Charafe-Jauffret E and Ginestier C: Brief reports: A distinct DNA methylation signature defines breast cancer stem cells and predicts cancer outcome. *Stem Cells* 32: 3031-3036, 2014.
10. Subramaniam D, Thombre R, Dhar A and Anant S: DNA methyltransferases: A novel target for prevention and therapy. *Front Oncol* 4: 80, 2014.
11. Baylin SB and Jones PA: A decade of exploring the cancer epigenome-biological and translational implications. *Nat Rev Cancer* 11: 726-734, 2011.
12. Baylin SB and Jones PA: Epigenetic determinants of cancer. *Cold Spring Harb Perspect Biol* 8: a019505, 2016.
13. Kok-Sin T, Mokhtar NM, Ali Hassan NZ, Sagap I, Mohamed Rose I, Harun R, Jamal R and Jamal R: Identification of diagnostic markers in colorectal cancer via integrative epigenomics and genomics data. *Oncol Rep* 34: 22-32, 2015.
14. Church TR, Wandell M, Lofton-Day C, Mongin SJ, Burger M, Payne SR, Castañón-Vélez E, Blumenstein BA, Rösch T, Osborn N, *et al*: Prospective evaluation of methylated SEPT9 in plasma for detection of asymptomatic colorectal cancer. *Gut* 63: 317-325, 2014.
15. Chen WD, Han ZJ, Skoletsky J, Olson J, Sah J, Myeroff L, Platzer P, Lu S, Dawson D, Willis J, *et al*: Detection in fecal DNA of colon cancer-specific methylation of the nonexpressed vimentin gene. *J Natl Cancer Inst* 97: 1124-1132, 2005.
16. Chen XY, Zhang J and Zhu JS: The role of m6A RNA methylation in human cancer. *Mol Cancer* 18: 103, 2019.
17. Zhang BY, Han L, Tang YF, Zhang GX, Fan XL, Zhang JJ, Xue Q and Xu ZY: METTL14 regulates M6A methylation-modified primary miR-19a to promote cardiovascular endothelial cell proliferation and invasion. *Eur Rev Med Pharmacol Sci* 24: 7015-7023, 2020.
18. Chen X, Xu M, Xu X, Zeng K, Liu X, Pan B, Li C, Sun L, Qin J, Xu T, *et al*: METTL14-mediated N6-methyladenosine modification of SOX4 mRNA inhibits tumor metastasis in colorectal cancer. *Mol Cancer* 19: 106, 2020.
19. Gu C, Wang Z, Zhou N, Li G, Kou Y, Luo Y, Wang Y, Yang J and Tian F: Mettl14 inhibits bladder TIC self-renewal and bladder tumorigenesis through N6-methyladenosine of Notch1. *Mol Cancer* 18: 168, 2019.
20. Gong PJ, Shao YC, Yang Y, Song WJ, He X, Zeng YF, Huang SR, Wei L and Zhang JW: Analysis of N6-Methyladenosine methyltransferase reveals METTL14 and ZC3H13 as tumor suppressor genes in breast cancer. *Front Oncol* 10: 578963, 2020.
21. Zhang X, Li D, Jia C, Cai H, Lv Z and Wu B: METTL14 promotes tumorigenesis by regulating lncRNA OIP5-AS1/miR-98/ADAMTS8 signaling in papillary thyroid cancer. *Cell Death Dis* 12: 617, 2021.
22. Wang M, Liu J, Zhao Y, He R, Xu X, Guo X, Li X, Xu S, Miao J, Guo J, *et al*: Upregulation of METTL14 mediates the elevation of PERP mRNA N⁶ adenosine methylation promoting the growth and metastasis of pancreatic cancer. *Mol Cancer* 19: 130, 2020.
23. Weng H, Huang H, Wu H, Qin X, Zhao BS, Dong L, Shi H, Skibbe J, Shen C, Hu C, *et al*: METTL14 inhibits hematopoietic stem/progenitor differentiation and promotes leukemogenesis via mRNA m⁶A modification. *Cell Stem Cell* 22: 191-205.e9, 2018.
24. Xu L, Hu H, Zheng LS, Wang MY, Mei Y, Peng LX, Qiang YY, Li CZ, Meng DF, Wang MD, *et al*: ETV4 is a theranostic target in clear cell renal cell carcinoma that promotes metastasis by activating the pro-metastatic gene FOSL1 in a PI3K-AKT dependent manner. *Cancer Lett* 482: 74-89, 2020.
25. Bao YN, Cao X, Luo DH, Sun R, Peng LX, Wang L, Yan YP, Zheng LS, Xie P, Cao Y, *et al*: Urokinase-type plasminogen activator receptor signaling is critical in nasopharyngeal carcinoma cell growth and metastasis. *Cell Cycle* 13: 1958-1969, 2014.
26. Li G, Su Q, Liu H, Wang D, Zhang W, Lu Z, Chen Y, Huang X, Li W, Zhang C, *et al*: Frizzled7 promotes epithelial-to-mesenchymal transition and stemness via activating canonical Wnt/beta-catenin pathway in gastric cancer. *Int J Biol Sci* 14: 280-293, 2018.
27. Livak KJ and Schmittgen TD: Analysis of relative gene expression data using real-time quantitative PCR and the 2(-Delta Delta C(T)) method. *Methods* 25: 402-408, 2001.
28. Marisa L, de Reynies A, Duval A, Selves J, Gaub MP, Vescovo L, Etienne-Grimaldi MC, Schiappa R, Guenet D, Ayadi M, *et al*: Gene expression classification of colon cancer into molecular subtypes: Characterization, validation, and prognostic value. *PLoS Med* 10: e1001453, 2013.
29. Hu Y, Gaedcke J, Emons G, Beissbarth T, Grade M, Jo P, Yeager M, Chanock SJ, Wolff H, Camps J, *et al*: Colorectal cancer susceptibility loci as predictive markers of rectal cancer prognosis after surgery. *Genes Chromosomes Cancer* 57: 140-149, 2018.
30. Raap M, Gierendt L, Kreipe HH and Christgen M: Transcription factor AP-2beta in development, differentiation and tumorigenesis. *Int J Cancer* 149: 1221-1227, 2021.
31. Liu J, Liu Z, Li M, Tang W, Pratap UP, Luo Y, Altwegg KA, Li X, Zou Y, Zhu H, *et al*: Interaction of transcription factor AP-2 gamma with proto-oncogene PELP1 promotes tumorigenesis by enhancing RET signaling. *Mol Oncol* 15: 1146-1161, 2021.
32. Moore LD, Le T and Fan G: DNA methylation and its basic function. *Neuropsychopharmacology* 38: 23-38, 2013.
33. Krebs AR: Studying transcription factor function in the genome at molecular resolution. *Trends Genet* 37: 798-806, 2021.
34. Xu L, Huang TJ, Hu H, Wang MY, Shi SM, Yang Q, Lin F, Qiang YY, Mei Y, Lang YH, *et al*: The developmental transcription factor IRF6 attenuates ABCG2 gene expression and distinctively reverses stemness phenotype in nasopharyngeal carcinoma. *Cancer Lett* 431: 230-243, 2018.
35. Yang X, Zhang S, He C, Xue P, Zhang L, He Z, Zang L, Feng B, Sun J and Zheng M: METTL14 suppresses proliferation and metastasis of colorectal cancer by down-regulating oncogenic long non-coding RNA XIST. *Mol Cancer* 19: 46, 2020.
36. Bhoumik A and Ronai Z: ATF2: A transcription factor that elicits oncogenic or tumor suppressor activities. *Cell Cycle* 7: 2341-2345, 2008.
37. Yang J, Lin Y, Huang Y, Jin J, Zou S, Zhang X, Li H, Feng T, Chen J, Zuo Z, *et al*: Genome landscapes of rectal cancer before and after preoperative chemoradiotherapy. *Theranostics* 9: 6856-6866, 2019.
38. Bolli N, Avet-Loiseau H, Wedge DC, Van Loo P, Alexandrov LB, Martincorena I, Dawson KJ, Iorio F, Nik-Zainal S, Bignell GR, *et al*: Heterogeneity of genomic evolution and mutational profiles in multiple myeloma. *Nat Commun* 5: 2997, 2014.
39. Corcoran RB, Andre T, Atreya CE, Schellens JHM, Yoshino T, Bendell JC, Hollebecque A, McRee AJ, Siena S, Middleton G, *et al*: Combined BRAF, EGFR, and MEK inhibition in patients with BRAFV600E-Mutant colorectal cancer. *Cancer Discov* 8: 428-443, 2018.
40. Xu L, Lin Y, Chen X, Zheng L, Cheng Y, Hu J, Zheng B, Zhang B, Li G, Chi Z, *et al*: A mutational signature for colorectal cancer prognosis prediction: Associated with immune cell infiltration. *Clin Transl Med* 11: e414, 2021.
41. Kim AS, Bartley AN, Bridge JA, Kamel-Reid S, Lazar AJ, Lindeman NI, Long TA, Merker JD, Rai AJ, Rimm DL, *et al*: Comparison of laboratory-developed tests and FDA-approved assays for BRAF, EGFR, and KRAS testing. *JAMA Oncol* 4: 838-841, 2018.
42. Levine M: Transcriptional enhancers in animal development and evolution. *Curr Biol* 20: R754-R763, 2010.
43. Bulger M and Groudine M: Functional and mechanistic diversity of distal transcription enhancers. *Cell* 144: 327-339, 2011.
44. Petrykowska HM, Vockley CM and Elnitski L: Detection and characterization of silencers and enhancer-blockers in the greater CFTR locus. *Genome Res* 18: 1238-1246, 2008.
45. Vokes SA, Ji H, Wong WH and McMahon AP: A genome-scale analysis of the cis-regulatory circuitry underlying sonic hedgehog-mediated patterning of the mammalian limb. *Genes Dev* 22: 2651-2663, 2008.
46. Ayer S and Benayati C: Conserved enhancer and silencer elements responsible for differential Adh transcription in Drosophila cell lines. *Mol Cell Biol* 10: 3512-3523, 1990.
47. Gaszner M and Felsenfeld G: Insulators: exploiting transcriptional and epigenetic mechanisms. *Nat Rev Genet* 7: 703-713, 2006.
48. Ohtsuki S, Levine M and Cai HN: Different core promoters possess distinct regulatory activities in the Drosophila embryo. *Genes Dev* 12: 547-556, 1998.
49. Calhoun VC, Stathopoulos A and Levine M: Promoter-proximal tethering elements regulate enhancer-promoter specificity in the Drosophila Antennapedia complex. *Proc Natl Acad Sci USA* 99: 9243-9247, 2002.

50. Spitz F and Furlong EE: Transcription factors: From enhancer binding to developmental control. *Nat Rev Genet* 13: 613-626, 2012.
51. Field A and Adelman K: Evaluating enhancer function and transcription. *Annu Rev Biochem* 89: 213-234, 2020.
52. Shannon M, Hamilton AT, Gordon L, Branscomb E and Stubbs L: Differential expansion of zinc-finger transcription factor loci in homologous human and mouse gene clusters. *Genome Res* 13: 1097-1110, 2003.
53. Yang L, Han Y, Suarez Saiz F and Minden MD: A tumor suppressor and oncogene: The WT1 story. *Leukemia* 21: 868-876, 2007.
54. Das Mandal S and Ray PS: Transcriptome-wide analysis reveals spatial correlation between N6-methyladenosine and binding sites of microRNAs and RNA-binding proteins. *Genomics* 113: 205-216, 2021.
55. Li B, Wang X, Li Z, Lu C, Zhang Q, Chang L, Li W, Cheng T, Xia Q and Zhao P: Transcriptome-wide analysis of N6-methyladenosine uncovers its regulatory role in gene expression in the lepidopteran *Bombyx mori*. *Insect Mol Biol* 28: 703-715, 2019.
56. Zhou H, Yin K, Zhang Y, Tian J and Wang S: The RNA m6A writer METTL14 in cancers: Roles, structures, and applications. *Biochim Biophys Acta Rev Cancer* 1876: 188609, 2021.



Copyright © 2024 Xu et al. This work is licensed under a Creative Commons Attribution-NonCommercial-NoDerivatives 4.0 International (CC BY-NC-ND 4.0) License.